Realization of chiral symmetry in the domain model of QCD

Alex C. Kalloniatis*
Special Research Centre for the Subatomic Structure of Matter, University of Adelaide, South Australia 5005, Australia

Sergei N. Nedelko†
Institute of Theoretical Physics III of Erlangen-Nuremberg University, Erlangen, Germany
and Bogoliubov Laboratory of Theoretical Physics, JINR, 141980 Dubna, Russia
(Received 27 November 2003; published 28 April 2004)

The domain model for the QCD vacuum has previously been developed and shown to exhibit confinement of quarks, a strong correlation of the local chirality of quark modes, and a duality of the background domain-like gluon field. Quark fluctuations satisfy a chirality violating boundary condition parametrized by a random chiral angle α_j on the jth domain. The free energy of an ensemble of $N\to\infty$ domains depends on $\{\alpha_j, j=1,\ldots,N\}$ through the logarithm of the quark determinant. Its parity odd part is given by the axial anomaly. The anomaly contribution to the free energy suppresses continuous axial $U(1)$ degeneracy in the ground state, leaving only a residual axial $Z(2)$ symmetry. This discrete symmetry and the flavor $SU(N_f)_L\times SU(N_f)_R$ chiral symmetry in turn are spontaneously broken with a quark condensate arising due to the asymmetry of the spectrum of the Dirac operator. In order to illustrate the splitting between the η' from octet pseudoscalar mesons realized in the domain model, we estimate the masses of the light pseudoscalar and vector mesons.

DOI: 10.1103/PhysRevD.69.074029 PACS number(s): 12.38.Aw, 12.38.Lg, 14.65.Bt, 14.70.Dj

I. INTRODUCTION

A mechanism that simultaneously provides for confinement of color, spontaneously broken chiral symmetry, and a resolution of the $U_A(1)$ problem remains one of the open problems in QCD today. Partial solutions [1] based on specific semiclassical or topologically stable configurations can go some way to manifest this triplet of phenomena, but founder either on generating all three or in allowing for an effective model of the vacuum from which hadron spectroscopy can be derived. In any case, one expects that topological objects of various dimensions—pointlike, stringlike, and sheetlike—should contribute [2], complete with significant quantum fluctuations, in a way that would be difficult to describe via an interacting microscopic model. In this paper, we continue the exploration of the ''domain model'' for the vacuum, originally proposed in [3], as a scenario for simultaneous appearance of all three phenomena: confinement, spontaneous chiral symmetry breaking via the appearance of a quark condensate, and a continuous $SU(N_f)_L\times SU(N_f)_R$ degeneracy of the vacuum for N_f massless quarks, but without a $U_A(1)$ continuous degeneracy of ground states that would be indicative of an unwanted Goldstone boson. The purpose of studying a model of this type is to identify the typical features of the relevant nonperturbative gluonic configurations. Such configurations would provide for as many gross features of nonperturbative QCD as possible. But the model should preserve simultaneously the well-studied short distance regime and should be expressed in terms of quark-gluon degrees of freedom as well as in terms of colorless hadron bound states.

The model under consideration provides for confinement of both static (area law) and dynamical (propagators are entire functions of momentum) quarks [3]. It also displays specific chiral properties of quark eigenmodes; namely, as will be discussed in more detail below, the spectrum of the Dirac operator is asymmetric with respect to $\lambda\to-\lambda$ and zero quark modes are absent, but the local chirality of all nonzero modes at the center of domains is correlated with the duality of the background field [4]. This has been observed on the lattice [5] and is usually considered as an indication of spontaneous breakdown of flavor chiral symmetry. The purpose of this article is to study the details of chiral symmetry realization in the domain model. The nonzero quark condensate and axial anomaly are generated as a result of spectral asymmetry and the definite mean chirality of the eigenmodes. We compute the quark condensate, study the degeneracies of the minima of the free energy of the domain ensemble with respect to chiral transformations, and estimate the spectrum of pseudoscalar mesons.

The model is defined by a partition function describing an ensemble of hyperspherical domains, each characterized by a background covariantly constant self-dual or anti-self-dual gluon field of random orientation. Summing over all orientations and both self-dual and anti-self-dual fields guarantees Lorentz and *CP* invariance. Quarks are confined as demonstrated in the original work [3]. On the boundaries of each hypersphere, fermion fluctuations satisfy a chirality violating boundary condition

$$i\not{\eta}(x)e^{i\alpha\gamma_5}\psi(x)=\psi(x) \tag{1}$$

which is 2π periodic in the chiral angle α. Here η_μ is a unit radial vector at the boundary. Integrating over all such chiral angles guarantees chiral invariance of the ensemble. As a consequence of Eq. (1), the spectrum of eigenvalues λ of the Dirac operator in a single domain is asymmetric under $\lambda\to-\lambda$. Such asymmetries have been studied in other con-

*Electronic address: akalloni@physics.adelaide.edu.au
†Electronic address: nedelko@thsun1.jinr.ru

texts, for example, by [6]. In the case of the domain model, the above boundary conditions are combined with the (anti-) self-dual gluon field which leads to a strong correlation between the local chirality of quark modes at the centers of domains with the duality of the background gluon field [4]. In this paper, we study how these aspects contribute to quark condensate formation and the pattern of chiral symmetry breaking.

The vacua of the quantum problem associated with an ensemble of domains are the minima of the free energy determined from the partition function. The problem of the quark contributions to the free energy requires calculation of the determinant of the Dirac operator in the presence of chirality violating boundary conditions. For a choice of boundary condition with $\alpha \to -i\vartheta - \pi/2$ this problem was tackled in [7] without taking into account the spectral asymmetry, where the parity odd part of the logarithm of the determinant was identified as $\ln\det(i\not{D}) \sim 2q\vartheta$ with q the topological charge (not necessarily integer) of the underlying gluon field, namely, the axial anomaly.

Our first goal in this paper is to address the analogous problem for the specific gluon field relevant to the domain model, taking into account the asymmetry of the spectrum. For the parity odd part we obtain

$$\ln\det(i\not{D}) \sim 2iq(\alpha \mod \pi). \tag{2}$$

This result is consistent with [7] up to a contribution coming from the asymmetry spectral function. However, we obtain an additional parity even part which also turns out to be α dependent. We consider this to be more an artifact of the incompleteness of our calculation than an established property of the determinant.

In the partition function all possible sets of chiral angles $\{\alpha_1, \ldots, \alpha_N\}$ are summed, ensuring the chiral invariance of the ensemble. Summation over all degrees of freedom in addition to chiral angles defines the free energy as a function of these chiral angles. In the limit $N \to \infty$ the minima of the free energy density in $\{\alpha_1, \ldots, \alpha_N\}$ determine the preferred chiral angles. More specifically, when self-dual and anti-self-dual configurations are summed, the anomaly Eq. (2) leads to a contribution to the free energy of the form $-\ln\cos[2q \arctan(\tan\alpha)]$ which vanishes when $\alpha = 0, \pi$. The minima are degenerate with respect to discrete Z_2 chiral transformations. Each of these minima are characterized by a quark condensate of opposite sign, which arises due to the spectral asymmetry. An infinitesimally small quark mass removes the degeneracy between the two discrete minima, and a nonzero quark condensate is generated with the value

$$\langle \bar{\psi}(x)\psi(x)\rangle = -(237.8 \text{ MeV})^3$$

with no additional modifications of the two model parameters after fixing in the gluonic sector of the theory. This gives a model with the chiral Z_2 discrete subgroup of $U_A(1)$ being spontaneously broken, and not the continuous $U_A(1)$ itself. In the absence of the mass term the ensemble average of $\bar{\psi}\psi$ correctly vanishes. A similar argument based on minimization of the free energy and thereby a relaxation of the effective θ parameter of QCD to zero is discussed in detail in [8] in the context of the strong *CP* problem.

Moreover, the form of Eq. (2) means that the free energy does not depend on flavor nonsinglet chiral angles when more than one massless quark flavors are introduced. This allows for the correct degeneracy of vacua with respect to continuous $SU(N_f)_L \times SU(N_f)_R$ chiral transformations. This vacuum structure implies the existence of Goldstone bosons in the flavor nonsinglet pseudoscalar channel but not in the singlet channel. To unveil more explicitly the singlet-octet splitting, we analyze the structure of pseudoscalar correlation functions in the context of the domain model and estimate the masses of light pseudoscalar and vector mesons. The qualitative conclusion of this analysis is that the area law (confinement of static quarks) and the singlet-octet splitting in the model have the same origin: the finite range correlations of the background gluon field.

In the next section we briefly review the model, followed by a summary of the properties of the spectrum of the Dirac operator in the domainlike gluon field. We then discuss in detail the calculation of the logarithm of the quark determinant for one massless quark flavor, including the role of spectral asymmetry in domains in giving the anomaly for the parity odd part. This is followed by an analysis of the symmetries of the ground state of the domain ensemble and the computation of the condensate. In Sec. V we generalize the result to N_f massless flavors in order to verify the spontaneous breaking of $SU(N_f)_L \times SU(N_f)_R$ in the ensemble. The last section is devoted to calculation of meson masses. Details of calculations are relegated to the Appendix.

II. THE DOMAIN MODEL

For motivation and a detailed description of the model we refer the reader to [3]. The essential definition of the model is given in terms of the following partition function for $N \to \infty$ domains of radius R:

$$\begin{aligned}\mathcal{Z} = \mathcal{N} \lim_{V,N\to\infty} \prod_{i=1}^{N} \int_{\Sigma} d\sigma_i \int_{\mathcal{F}^i_\psi} \mathcal{D}\psi^{(i)}\mathcal{D}\bar{\psi}^{(i)} \\ \times \int_{\mathcal{F}^i_Q} \mathcal{D}Q^i \delta[D(\check{B}^{(i)})Q^{(i)}]\Delta_{\mathrm{FP}}[\check{B}^{(i)}, Q^{(i)}] \\ \times e^{-S^{\mathrm{QCD}}_{V_i}[Q^{(i)}+\check{B}^{(i)}, \psi^{(i)}, \bar{\psi}^{(i)}]}\end{aligned} \tag{3}$$

where the functional spaces of integration $\mathcal{F}^i_Q$ and $\mathcal{F}^i_\psi$ are specified by the boundary conditions $(x - z_i)^2 = R^2$

$$\check{n}_i Q^{(i)}(x) = 0, \tag{4}$$

$$i\not{n}_i(x) e^{i\alpha_i\gamma_5}\psi^{(i)}(x) = \psi^{(i)}(x), \tag{5}$$

$$\bar{\psi}^{(i)} e^{i\alpha_i\gamma_5} i\not{n}_i(x) = -\bar{\psi}^{(i)}(x). \tag{6}$$

Here $\check{n}_i = n^a_i t^a$ with the generators t^a of $SU_{\mathbf{c}}(3)$ in the adjoint representation and the α_i are chiral angles associated with the boundary condition Eq. (5) with different values randomly assigned to domains. We shall discuss this constraint

in detail in later sections. The thermodynamic limit assumes $V,N\to\infty$ but with the density $v^{-1}=N/V$ taken fixed and finite. The partition function is formulated in a background field gauge with respect to the domain mean field, which is approximated inside and on the boundaries of the domains by a covariantly constant (anti-)self-dual gluon field with the field-strength tensor of the form

$$F^a_{\mu\nu}(x)=\sum_{j=1}^{N} n^{(j)a}B^{(j)}_{\mu\nu}\vartheta(1-(x-z_j)^2/R^2),$$

$$B^{(j)}_{\mu\nu}B^{(j)}_{\mu\rho}=B^2\delta_{\nu\rho}.$$

Here z^μ_j are the positions of the centers of domains in Euclidean space.

The measure of integration over parameters characterizing domains is

$$\int_\Sigma d\sigma_i \ldots = \frac{1}{48\pi^2}\int_V \frac{d^4z_i}{V}\int_0^{2\pi} d\alpha_i \int_0^{2\pi} d\varphi_i \int_0^{\pi} d\vartheta_i \sin\theta_i \times \int_0^{2\pi} d\xi_i \sum_{l=0,1,2}^{3,4,5} \delta\left(\xi_i-\frac{(2l+1)\pi}{6}\right) \times \int_0^{\pi} d\omega_i \sum_{k=0,1} \delta(\omega_i-\pi k)\ldots, \quad (7)$$

where (θ_i,φ_i) are the spherical angles of the chromomagnetic field, ω_i is the angle between chromoelectric and chromomagnetic fields, and ξ_i is an angle parametrizing the color orientation.

This partition function describes a statistical system of the domainlike structures of density v^{-1} where the volume of a domain is $v=\pi^2R^4/2$. Each domain is characterized by a set of internal parameters and whose internal dynamics are represented by fluctuation fields. Most of the symmetries of the QCD Lagrangian are respected, since the statistical ensemble is invariant under space-time and color gauge transformations. For the same reason, if the quarks are massless then the chiral invariance is respected. The model involves only two free parameters: the mean field strength B and the mean domain radius R. These dimensionful parameters break the scale invariance present originally in the QCD Lagrangian. In principle, they should be related to the trace anomaly of the energy-momentum tensor [9,10] and, eventually, to the fundamental scale $\Lambda_{\rm QCD}$. Knowledge of the full quantum effective action of QCD would be required for establishing a relation of this kind.

A straightforward application of Eq. (3) to the vacuum expectation value of a product of n field strength tensors, each of the form

$$B^a_{\mu\nu}(x)=\sum_j n^{(j)a}B^{(j)}_{\mu\nu}\theta(1-(x-z_j)^2/R^2),$$

gives for the connected n-point correlation function

$$\langle B^{a_1}_{\mu_1\nu_1}(x_1)\cdots B^{a_n}_{\mu_n\nu_n}(x_n)\rangle = \lim_{V,N\to\infty}\sum_j^N \int_V \frac{dz_j}{V}\int d\sigma_j n^{(j)a_1}\cdots n^{(j)a_n}B^{(j)}_{\mu_1\nu_1}\cdots B^{(j)}_{\mu_n\nu_n}\theta(1-(x_1-z_j)^2/R^2)\cdots\theta(1-(x_n-z_j)^2/R^2) = B^n t^{a_1\cdots a_n}_{\mu_1\nu_1,\ldots,\mu_n\nu_n}\Xi_n(x_1,\ldots,x_n),$$

where the tensor t is given by the integral

$$t^{a_1\cdots a_n}_{\mu_1\nu_1,\ldots,\mu_n\nu_n}=\int d\sigma_j n^{(j)a_1}\cdots n^{(j)a_n}B^{(j)}_{\mu_1\nu_1}\cdots B^{(j)}_{\mu_n\nu_n},$$

and can be calculated explicitly using the measure Eq. (7). This tensor vanishes for odd n. In particular, the integral over spatial directions is defined by the generating formula

$$\frac{1}{4\pi}\int_0^{2\pi} d\varphi_j\int_0^{\pi} d\theta_j \sin\theta_j e^{B^{(j)}_{\mu\nu}J_{\mu\nu}} = \frac{\sin\sqrt{2B^2[J_{\mu\nu}J_{\mu\nu}\pm\tilde{J}_{\mu\nu}J_{\mu\nu}]}}{\sqrt{2B^2[J_{\mu\nu}J_{\mu\nu}\pm\tilde{J}_{\mu\nu}J_{\mu\nu}]}}.$$

The translation-invariant function

$$\Xi_n(x_1,\ldots,x_n)=\frac{1}{v}\int d^4z\,\theta(1-(x_1-z)^2/R^2)\cdots\theta(1-(x_n-z)^2/R^2) \quad (8)$$

can be seen as the volume of the region of overlap of n hyperspheres of radius R and centers $(x_1,\ldots,x_n)$, normalized to the volume of a single hypersphere $v=\pi^2R^4/2$,

$$\Xi_n=1 \text{ for } x_1=\cdots=x_n.$$

It is obvious from this geometrical interpretation that Ξ_n is a continuous function and vanishes if the distance between any two points $|x_i-x_j|\geqslant 2R$; correlations in the background field have finite range $2R$. The Fourier transform of Ξ_n is then an entire analytical function, and thus the correlations do not have a particle interpretation. It should be stressed that the statistical ensemble of background fields is not Gaussian since all connected correlators are independent of each other and cannot be reduced to the two-point correlations.

Within this framework the gluon condensate to lowest order in fluctuations is $4B^2$, the absolute value of the topological charge per domain reads $q=B^2R^4/16$, and the topological susceptibility turns out to be $\chi=B^4R^4/128\pi^2$. An area law is obtained for static quarks. Computation of the Wilson loop for a circular contour of a large radius $L\gg R$ gives a string tension $\sigma=Bf(\pi BR^2)$ where f is given for color $SU(2)$ and $SU(3)$ in [3]. The area law emerges due to the finite range of background field correlators Eq. (48). On the other hand, the model cannot account for such a subtle feature as Casimir scaling: the adjoint Wilson loop naturally

shows perimeter law, but trivially because of the Abelian character of the domain mean field.

Estimations of the values of these quantities are known from lattice calculation or phenomenological approaches and can be used to fit B and R. As described in [3] these parameters are fixed to be $\sqrt{B}=947$ MeV, $R=(760\ \text{MeV})^{-1}=0.26$ fm with the average absolute value of topological charge per domain turning out to be $q\approx 0.15$ and the density of domains $v^{-1}=42\ \text{fm}^{-4}$. The topological susceptibility is then $\chi=(197\ \text{MeV})^4$, comparable to the Witten-Veneziano value [11]. This fixing of the parameters of the model remains unchanged in this investigation of the quark sector. The quark condensate at the origin of a domain where angular dependence drops out was estimated in paper [3] with the result of $-(228\ \text{MeV})^3$.

III. DIRAC OPERATOR AND SPECTRUM

The eigenvalue problem

$$\not{D}\psi(x)=\lambda\psi(x),$$

$$i\not{n}(x)e^{i\alpha\gamma_5}\psi(x)=\psi(x),\quad x^2=R^2$$

was studied in [4]. The dirac matrices are in an anti-Hermitian representation. For α assumed to be real a biorthogonal basis has to be constructed. Solutions can be labeled via the Casimirs and eigenvalues

$$\mathbf{K}_1^2=\mathbf{K}_2^2\rightarrow\frac{k}{2}\left(\frac{k}{2}+1\right),\quad k=0,1,\ldots,\infty,$$

$$K_{1,2}^z\rightarrow m_{1,2},$$

$$m_{1,2}=-k/2,\ -k/2+1,\ \ldots,\ k/2-1,\ k/2,$$

corresponding to the angular momentum operators

$$\mathbf{K}_{1,2}=\frac{1}{2}(\mathbf{L}\pm\mathbf{M})$$

with $\mathbf{L}$ the usual three-dimensional angular momentum operator and $\mathbf{M}$ the Euclidean version of the boost operator. The solutions for the self-dual background field are then

$$\psi_{km_1}^{-\kappa}=i\not{n}\chi_{km_1}^{-\kappa}+\varphi_{km_1}^{-\kappa},\tag{9}$$

where χ and φ must both have negative chirality in the self-dual field and κ is related to the polarization of the field defined via the projector

$$O_\kappa=N_+\Sigma_\kappa+N_-\Sigma_{-\kappa}\tag{10}$$

with

$$N_\pm=\frac{1}{2}(1\pm\hat{n}/|\hat{n}|),\quad \Sigma_\pm=\frac{1}{2}(1\pm\boldsymbol{\Sigma}\mathbf{B}/B)$$

being respectively separate projectors for color and spin polarizations. Significantly, the negative chirality for χ and φ is the only choice for which the boundary condition Eq. (5) can be implemented for the self-dual background. The explicit form of the spinors χ and φ can be found in [4], where it is demonstrated that the eigenspinor Eq. (9) has definite chirality at the center of domains correlated with the duality of the gluon field. The boundary condition reduces to

$$\chi=-e^{\mp i\alpha}\varphi,\quad \overline{\chi}=\overline{\varphi}e^{\mp i\alpha},\quad x^2=R^2,\tag{11}$$

where upper (lower) signs correspond to $\varphi(\chi)$ with chirality ∓ 1, which, using the solutions, amounts to equations for the two possible polarizations, for Λ_k^{-+}:

$$e^{-i\alpha}M(k+2-\Lambda^2,k+2,z_0)-\frac{\sqrt{z_0}}{i\Lambda}\Bigg[M(k+2-\Lambda^2,k+2,z_0)-\frac{k+2-\Lambda^2}{k+2}M(k+3-\Lambda^2,k+3,z_0)\Bigg]=0,\tag{12}$$

and for Λ_k^{--}:

$$e^{-i\alpha}M(-\Lambda^2,k+2,z_0)+\frac{i\Lambda\sqrt{z_0}}{k+2}M(1-\Lambda^2,k+3,z_0)=0,\tag{13}$$

where $z_0=\hat{B}R^2/2$ and $\Lambda=\lambda/\sqrt{2\hat{B}}$. For the present work Eqs. (12), (13) are the starting point, from which we see by inspection that a discrete spectrum of complex eigenvalues emerges for which there is no symmetry of the form $\lambda\rightarrow-\lambda$. For given chirality and polarization and angular momentum k, an infinite set of discrete Λ are obtained labeled by a "principal quantum number" n.

IV. QUARK DETERMINANT AND FREE ENERGY FOR A SINGLE DOMAIN

A. Massless case

We consider the one-loop contribution of the quarks to the free energy density $F(B,R|\alpha)$ of a single (anti-)self-dual domain of volume $v=\pi^2R^4/2$,

$$\exp\{-vF(B,R|\alpha)\}=\det{}_\alpha\left(\frac{i\not{D}}{i\not{\partial}}\right)=\prod_{\kappa,k,n,m_1}\left(\frac{\lambda_{kn}^\kappa(B)}{\lambda_{kn}^\kappa(0)}\right)=\exp\{-\zeta'(s)\}_{s=0}.\tag{14}$$

The normalization is chosen such that $\lim_{B\rightarrow 0}F(B,R|\alpha)=0$. The free energy is then $F=v^{-1}\zeta'(0)$.

In the zeta-regularized determinant an arbitrary scale μ appears, and it is convenient to work with scaled variables

$$\beta=\sqrt{2\hat{B}}/\mu,\quad \rho=\mu R,\quad \xi=\lambda(B)/\mu,\quad \xi_0=\lambda(0)/\mu,$$

and where the dimensionless quantity $z=BR^2/2=\beta^2\rho^2/4$ appears prominently. Moreover, it is convenient to analytically

continue $\alpha \to -i\vartheta - \pi/2$ to guarantee a real spectrum of eigenvalues of the Dirac operator for all ϑ. We shall regard the background domain field as being self-dual in the following. Then, Eqs. (12), (13) can be recast into a form determining the rescaled eigenvalues ξ, namely,

$$M(k+2-\xi^2/\beta^2,k+2,z)+e^{\vartheta}\frac{\beta^2\rho}{2\xi}\Bigg[M(k+2-\xi^2/\beta^2,k+2,z) - \frac{k+2-\xi^2/\beta^2}{k+2}M(k+3-\xi^2/\beta^2,k+3,z)\Bigg]=0 \tag{15}$$

for ξ^{-+} and

$$M(-\xi^2/\beta^2,k+1,z)+e^{\vartheta}\frac{\xi\rho}{2(k+1)}M(1-\xi^2/\beta^2,k+2,z)=0 \tag{16}$$

for ξ^{--}. The zeta function $\zeta(s)$ breaks up into two parts [6], respectively symmetric (S) and antisymmetric (AS) with respect to $\xi \to -\xi$:

$$\zeta(s)=\zeta_{\mathrm{S}}(s)+\zeta_{\mathrm{AS}}(s),$$

with

$$\zeta_{\mathrm{S}}(s)=\frac{1}{2}(1+e^{\mp i\pi s})\zeta_{\mathbb{D}^2}(s/2), \tag{17}$$

$$\zeta_{\mathrm{AS}}(s)=\frac{1}{2}(1-e^{\mp i\pi s})\eta(s). \tag{18}$$

The assumption behind these representations is that the spectrum of eigenvalues can be well ordered according to the magnitude of the eigenvalues $|\xi|$, which is certainly the case with the solutions to Eqs. (15), (16). However, there is an ambiguity which can be fixed by specifying whether the smallest-in-magnitude eigenvalue is either positive or negative. This determines correspondingly the sign choice in Eqs. (17), (18).

Thus the key quantities devolve into the zeta function for the squared Dirac operator and the asymmetry function, respectively:

$$\zeta_{\mathbb{D}^2}(s)=\sum_{k,n,\kappa}(k+1)\left(\frac{1}{[\xi^{\kappa}_{kn}(B)]^{2s}}-\frac{1}{[\xi^{\kappa}_{kn}(0)]^{2s}}\right), \tag{19}$$

$$\eta(s)=\sum_{k,n,\kappa}(k+1)\left(\frac{\mathrm{sgn}[\xi^{\kappa}_{kn}(B)]}{|\xi^{\kappa}_{kn}(B)|^{s}}-\frac{\mathrm{sgn}[\xi^{\kappa}_{kn}(0)]}{|\xi^{\kappa}_{kn}(0)|^{s}}\right). \tag{20}$$

It should be stressed that in the presence of baglike boundary conditions ζ_{S} and ζ_{AS} do not have the meaning of parity conserving and parity violating terms since a parity transformation in terms of eigenvalues is given by $\xi(\vartheta)\to -\xi(-\vartheta)$ and both spectral functions contain parity conserving and violating terms. Thus the determinant for a given parameter ϑ is defined by

$$\zeta'(0)=\left(\frac{1}{2}\zeta'_{\mathbb{D}^2}(0)\pm i\frac{\pi}{2}\zeta_{\mathbb{D}^2}(0)\mp i\frac{\pi}{2}\eta(0)\right), \tag{21}$$

with the normalization chosen in Eq. (14) such that $\zeta'(0)$ vanishes as $B\to 0$.

The spectral sums over quantum labels N can be computed using a representation of the sum as a contour integral of the logarithmic derivative of the function whose zeros determine the spectrum,

$$\sum_{N}\frac{1}{\xi_N^s}=\frac{1}{2\pi i}\oint_{\Gamma}\frac{d\xi}{\xi^s}\frac{d}{d\xi}\ln f(\xi) \tag{22}$$

(see [12]), where the zeros of $f(\xi)=0$ are $\xi=\xi_N$ and the contour is chosen such that all zeros are enclosed. With a real parameter ϑ, the poles lie on the real axis, and there is no pole at the origin for any ϑ. By deforming the contour and accounting for the vanishing of contributions to the integral at infinity, the expressions arising from Eq. (22) can be transformed into real integrals. The following representations for the two spectral functions are eventually obtained:

$$\zeta_{\mathbb{D}^2}(s)=\rho^{2s}\frac{\sin(\pi s)}{\pi}\sum_{k=1}^{\infty}k^{1-2s}\int_0^{\infty}\frac{dt}{t^{2s}}\frac{d}{dt}\Psi(k,t|z,\vartheta),$$

$$\eta(s)=\rho^{s}\frac{\cos(\pi s/2)}{i\pi}\sum_{k=1}^{\infty}k^{1-s}\int_0^{\infty}\frac{dt}{t^{s}}\frac{d}{dt}\Phi(k,t|z,\vartheta), \tag{23}$$

with Ψ and Φ being the sums of contributions from the two polarizations, taking the forms

$$\Psi(k,t|z,\vartheta)=\sum_{\kappa=\pm}\ln\left(\frac{A^2_{\kappa}(k,t|z)+e^{2\vartheta}B^2_{\kappa}(k,t|z)}{A^2(k,t)+e^{2\vartheta}B^2(k,t)}\right),$$

$$\Phi(k,t|z,\vartheta)=\sum_{\kappa=\pm}\ln\left(\frac{A_{\kappa}(k,t|z)+ie^{\vartheta}B_{\kappa}(k,t|z)}{A_{\kappa}(k,t|z)-ie^{\vartheta}B_{\kappa}(k,t|z)}\right),$$

and where

$$A_{-}(k,t|z)=M\left(\frac{k^2t^2\rho^2}{4z},k+1,z\right),$$

$$B_{-}(k,t|z)=\frac{kt\rho}{2(k+1)}M\left(1+\frac{k^2t^2\rho^2}{4z},k+2,z\right),$$

$$A_{+}(k,t|z)=M\left(-\frac{k^2t^2\rho^2}{4z},k+1,-z\right),$$

$$B_{+}(k,t|z)=\frac{2z}{kt\rho}\Bigg[M\left(-\frac{k^2t^2\rho^2}{4z},k+1,-z\right) - \frac{k+1+k^2t^2\rho^2/4z}{k+1}M\left(-\frac{k^2t^2\rho^2}{4z},k+2,-z\right)\Bigg],$$

$$A(k,t)=\frac{2^k k!}{(kt\rho)^k}I_k(kt\rho),$$

$$B(k,t)=\frac{2^k k!}{(kt\rho)^k}I_{k+1}(kt\rho). \tag{24}$$

The Bessel functions I_k emerge from the limit $B\to 0$ with the normalization of the determinant as specified above. The next step is to expand the confluent hypergeometric functions in $1/k$, similar to the Debye expansion of Bessel functions, for example,

$$M\left(\frac{k^2t^2\rho^2}{4z},k+1,z\right)=C(t\rho,k)\sum_{n=0}^{\infty}\frac{M_n(t\rho,z)}{k^n}. \tag{25}$$

The forms of the prefactors and the $M_n(x,z)$ functions are given in the Appendix for the various Kummer functions appearing in A_κ and B_κ.

Before proceeding with more detail, let us give an overview of the subsequent steps. The expansions Eq. (25) are first inserted in $\zeta(s)$ and $\eta(s)$. Then the integrals over t can be evaluated term by term in the series in $1/k$. The order of summation over k and n is then exchanged. This is the most subtle step, which we discuss below. But it means that now the sums over k can be read off in terms of the Riemann zeta function. The resulting $\zeta_{\mathbb{D}^2}(s)$ then has the structure

$$\zeta_{\mathbb{D}^2}(s)=s\rho^{2s}\frac{\sin(\pi s)}{i\pi}\sum_{n=0}^{\infty}\zeta_{\mathrm{R}}(2s+n-1)f(z^2|n)+\delta\zeta_{\mathbb{D}^2}(s), \tag{26}$$

where the term $\delta\zeta$ denotes those potentially present contributions coming from interchange of the order of summations over n and k. A similar structure appears for the asymmetry spectral function as well. Then we are interested in the decomposition of the resulting expressions around $s=0$. In this limit the first term in Eq. (26) provides only a contribution from the $n=2$ term and can be calculated with relative ease since only the lowest coefficients M_1 and M_2 in Eq. (25) contribute. However, as occurs in even simple problems [13], the second term in Eq. (26) is much more difficult to compute. To achieve this one needs to know the coefficients $f(z^2|n)$ as a function of the continuous variable n. Below we will elucidate the contribution from the first term alone, bearing in mind the necessity of a complete analysis.

Now, in more detail, using expansions of the type Eq. (25) as given in the Appendix, we arrive at the following expansions of Ψ and Φ in $1/k$:

$$\Psi(k,t|z,\vartheta)=z^2\left[\frac{\Psi_1(y)}{k}+\frac{\Psi_2(y|\vartheta)}{k^2}\right]+O(1/k^3),$$

$$\Phi(k,t|z,\vartheta)=z^2\frac{\Phi_2(y|\vartheta)}{k^2}+O(1/k^3),$$

with the coefficient functions

$$\Psi_1(y)=-\frac{2}{3}\frac{y(y-1)(3y+1)}{(y+1)^2},$$

$$\begin{aligned}\Psi_2(y|\vartheta)=&\frac{y^2(y-1)}{[y+1-(y^2-1)^2e^{2\vartheta}]^2}\\&\times[(y^2-1)(2y^3+6y^2+7y+1)\\&-2(y+1)(2y^4+5y^3+5y^2-y+1)e^{2\vartheta}\\&+(y-1)(2y^4+6y^3+5y^2-4y-1)e^{4\vartheta}],\end{aligned}$$

$$\Phi_2(y|\vartheta)=-2ie^{\vartheta}y^2\sqrt{1-y^2}\,\frac{(1-y)^2e^{2\vartheta}-(1+y)^2}{[1+y+(1-y)e^{2\vartheta}]^2},$$

with $y=1/\sqrt{1+t^2}$. We thus get for $s\ll 1$

$$\zeta_{\mathbb{D}^2}(s)=z^2(1+2s\ln\rho)s\left[-\frac{1}{2}\mathcal{I}_1+\left(\frac{1}{2s}+\gamma\right)\mathcal{I}_2\right],$$

$$\mathcal{I}_1=\int_0^\infty\frac{dt}{t^{2s}}\frac{d}{dt}\Psi_1(y)=-s+O(s^2),$$

$$\begin{aligned}\mathcal{I}_2=&\int_0^\infty\frac{dt}{t^{2s}}\frac{d}{dt}\Psi_2(y|\vartheta)\\=&2s\left[-\frac{1}{4}-\ln 2+\ln(1+e^{2\vartheta})\right]+O(s^2),\end{aligned}$$

and

$$\eta(s)=-\frac{z^2}{i\pi}(1+s\ln\rho)\frac{1}{s}\mathcal{J}_2,$$

$$\begin{aligned}\mathcal{J}_2=&2ie^{\vartheta}\int_0^\infty\frac{dt}{t^s}\frac{d}{dt}\Phi_2(y|\vartheta)\\=&-s\frac{i}{2}[\pi+2\arctan(\sinh(\vartheta)]+O(s^2)\end{aligned}$$

upon performing the t (or y) integrations and where we have used that

$$\zeta_{\mathrm{R}}(0)=-\frac{1}{2},\quad \zeta_{\mathrm{R}}(1+2s)=\frac{1}{2s}+\gamma+O(s).$$

The final results for the first term in Eq. (26) and its analogue in the asymmetry function $\eta(s)$ are then summarized in the following equations:

$$\zeta_{\mathbb{D}^2}(0)=0,$$

$$\zeta'_{\mathbb{D}^2}(0)=z^2\left[-\frac{1}{4}-\ln 2+\ln(1+e^{2\vartheta})\right],$$

$$\eta(0)=\frac{z^2}{2}+\frac{z^2}{\pi}\arctan[\sinh(\vartheta)],$$

and hence

$$\zeta'(0)=\frac{z^2}{2}\Big[-\frac{1}{4}-\ln 2\pm i\frac{\pi}{2}+\ln(1+e^{2\vartheta})$$
$$\mp i\arctan[\sinh(\vartheta)]\Big]+\delta\zeta'(0). \tag{27}$$

Now we can straightforwardly continue $\vartheta\to i\alpha+i\pi/2$. The final result for the free energy F is complex with an imaginary part of the form

$$\Im F=\pm 2q\arctan[\tan(\alpha)] \tag{28}$$

where q is the absolute value of the topological charge in a domain. This charge is not integer here in general but the anomalous term is πn periodic in α. This is the Abelian anomaly as observed within the context of baglike boundary conditions by [7]. Its appearance here is in the spirit of the derivation by Fujikawa [14], where the phase appears as an extra contribution under a chiral transformation on the fermionic measure of integration.

However, the analytic continuation of Eq. (27) also exposes an α-dependent real part,

$$F(\alpha)=\frac{z^2}{2}\Big[-\frac{1}{4}+\ln[1\pm\cos(\alpha)]\Big],$$

where the signs are according to the prescription in Eqs. (17), (18). There is no reason to expect that anything other than the anomaly should appear in the logarithm of the determinant. Thus the likelihood is that this additional real part contribution should be canceled by the contributions $\delta\zeta$ in Eq. (26), which remains to be verified.

Below we assume that the anomaly Eq. (28) provides the entire result for the α-dependent part of the free energy of massless fermions in a domain, which leads to intriguing consequences.

B. Massive fermions

Inclusion of an infinitesimally small fermion mass leads to a modification of the free energy by a term which is linear in mass to leading order, namely [6],

$$F=F_{m=0}+i\frac{m}{\mu v}\eta(1). \tag{29}$$

Using again the representation Eq. (23) but now in the vicinity of $s=1$, one can find the following representation for the summed contributions of both polarizations in the self-dual domain to the asymmetry function:

$$\eta(s)=i\mu Re^{i\alpha}\frac{\cos(\pi s/2)}{\pi(1-s)}\sum_{k=1}^{\infty}k^{1-s}\frac{k}{k+1}\Big[-1+M(1,k+2,z)$$
$$-\frac{z}{k+2}M(1,k+3,-z)\Big]. \tag{30}$$

We next evaluate the asymptotic behavior in k. A singular term as $s\to 1$ can be extracted, which turns out to be independent of the field (that is, B) and is canceled by the normalization. The final expression for the free energy density for a self-dual domain, including the contribution linear in mass, is

$$F^{(\mathrm{sd})}=2iq\arctan[\tan(\alpha)]-e^{i\alpha}m\langle\bar\psi\psi\rangle,$$

where we have used the suggestive notation

$$\langle\bar\psi\psi\rangle=\frac{1}{\pi^2R^3}\sum_{k=1,z=z_1,z_1,z_2}^{\infty}\frac{k}{k+1}\Big[M(1,k+2,z)$$
$$-\frac{z}{k+2}M(1,k+3,-z)-1\Big] \tag{31}$$

coming from $\eta(1)$ with the sum over z corresponding to a color trace.

Let us summarize the results of this section as follows. The α-dependent part of the free energy of a self-dual domain for massive quarks is complex with the following real and imaginary parts:

$$F=\Re F+i\,\Im F,$$
$$\Re F=-m\cos\alpha\langle\bar\psi\psi\rangle, \tag{32}$$
$$\Im F=2\frac{q}{v}\arctan[\tan(\alpha)]-m\sin\alpha\langle\bar\psi\psi\rangle. \tag{33}$$

The free energy of an anti-self-dual domain is obtained via complex conjugation.

V. ENSEMBLE FREE ENERGY AND CHIRAL SYMMETRIES

A. One-flavor case: Quark condensate and $U_A(1)$

Under the assumption that only the anomalous term depends on the chiral angle, the part of the free energy density $\mathcal{F}$ relevant for the present consideration of an ensemble of $N\to\infty$ domains with both self-dual and anti-self-dual configurations takes the form

$$e^{-vN\mathcal{F}}=\mathcal{N}\prod_j^N\int_0^{2\pi}d\alpha_j\frac{1}{2}[e^{iv\Im F(\alpha_j)}+e^{-iv\Im F(\alpha_j)}]$$
$$=\mathcal{N}\prod_j^N\int_0^{2\pi}d\alpha_j e^{\ln\{\cos[v\Im F(\alpha_j)]\}}$$
$$=\mathcal{N}\exp(N\max_{\alpha}\ln\{\cos[v\Im F(\alpha)]\}).$$

The maxima (minima of the free energy density) are achieved at $\alpha_1=\cdots=\alpha_N=\pi n$.

In the absence of a quark mass, only the anomaly contribution in the imaginary part $\Im F$ of the free energy of a single

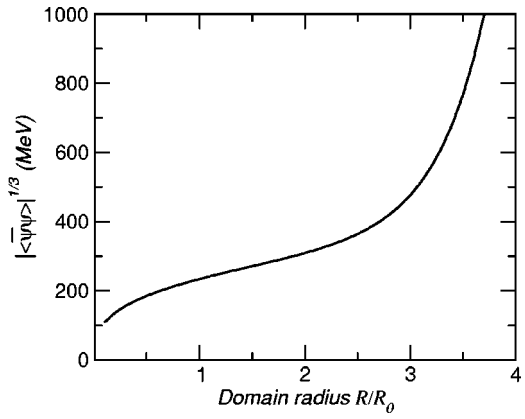

FIG. 1. Absolute value of quark condensate as a function of domain radius $[R_0=(760\ \mathrm{MeV})^{-1}]$.

domain appears under the logarithm of the cosine and defines the minima of the free energy density, $\ln\{\cos[v\mathfrak{F}F(\alpha)]\}=0$. Thus for massless quarks there is no continuous $U_A(1)$ symmetry in the ground states, rather a discrete Z_2 chiral symmetry. The anomaly plays a peculiar role here: selecting out those chiral angles which minimize the free energy so that the full $U_A(1)$ group is no longer reflected in the vacuum degeneracy. It should be stressed here that this residual discrete degeneracy is sufficient to ensure a zero value for the quark condensate in the absence of a mass term or some other external chirality violating sources.

Now, switching on the quark mass, we see this discrete symmetry spontaneously broken, and one of the two vacua selected in the infinite volume limit according to the sign of the mass. In this case (for these conventions of boundary condition and mass term), the minimum at $\alpha=0$ is selected. The quark condensate can now be extracted from the free energy via

$$\langle\bar{\psi}(x)\psi(x)\rangle=-\lim_{m\to 0}\lim_{N\to\infty}(vN)^{-1}\frac{d}{dm}e^{-vN\mathcal{F}(m)}.$$

Taking the thermodynamic limit $N\to\infty$ and then $m\to 0$ gives a nonzero condensate

$$\langle\bar{\psi}(x)\psi(x)\rangle=-\langle\bar{\psi}\psi\rangle. \tag{34}$$

According to Eq. (31) the condensate is equal to

$$\langle\bar{\psi}(x)\psi(x)\rangle=-(237.8\ \ \mathrm{MeV})^3 \tag{35}$$

for the values of field strength B and domain radius R fixed earlier by consideration of the pure gluonic characteristics of the vacuum—string tension, topological susceptibility, and gluon condensate. A nonzero condensate is generated without a continuous degeneracy of the ground states of the system.

Dependence of the condensate on the domain radius R is illustrated in Fig. 1. As expected, the condensate diverges with $R\to\infty$, since in this limit the number of low lying strongly chiral modes is growing. We will return to the discussion of this feature again in the section on the meson spectrum.

B. Multiflavor case: Spontaneous breakdown of $SU_{\mathrm{L}}(N_f)\times SU_{\mathrm{R}}(N_f)$

The question remains whether any continuous directions in the space of vacua are to be expected when the full flavor chiral symmetry is brought into play. For this we must generalize the analysis. We consider N_f massless quark flavors. First, we observe that the fermion boundary condition in Eq. (5) explicitly breaks all chiral symmetries, flavor singlet and nonsinglet (see also [7]). Thus the procedure we have used here of integrating over all α does not suffice to restore the full chiral symmetry of the massless QCD action. Rather, the boundary condition must be generalized to include flavor nonsinglet angles,

$$\alpha\to\alpha+\beta^a T^a,$$

with T^a the N_f^2-1 generators of $SU(N_f)$. Then integration over N_f^2 angles $\alpha,\beta^a\in[0,2\pi]$ must be performed for a fully chiral symmetric ensemble. The spectrum of the Dirac problem now proceeds quite analogously, except that the boundary condition mixes flavor components; thus an additional projection into flavor sectors is required in order to extract the eigenvalue equation analogous to Eq. (11).

For $N_f=2$ the boundary condition can be chosen as

$$i\not{n}(x)e^{i(\alpha+\vec{\beta}\cdot\vec{\sigma}/2)\gamma_5}\psi(x)=\psi(x), \tag{36}$$

where flavors now mix on the boundary. We must now solve the Dirac spectrum in the presence of this mixing. The spinors χ and φ used in our solutions now become isospin doublets. We need to project the boundary condition onto separate equations for eigenvalues.

Things proceed much as before in the spin sector with our previous decompositions and projectors. The boundary condition will devolve to the structure

$$\chi[\lambda]=e^{i(\alpha+\vec{\beta}\cdot\vec{\sigma}/2)}\varphi[\lambda],$$

where the γ_5 in the exponent is eliminated via the projection into chirality eigenspinors. The equation still mixes the flavor components and cannot be solved for an eigenvalue λ.

We introduce projectors

$$P_{\pm}(\beta)\equiv\frac{1\pm\hat{\beta}\cdot\vec{\sigma}}{2}$$

which have the property

$$P_{\pm}(\beta)e^{-i\vec{\beta}\cdot\vec{\sigma}/2}=e^{\pm i|\vec{\beta}|/2}P_{\pm}(\beta).$$

Note here the appearance of the magnitude of the triplet $\vec{\beta}$ in the exponent. Projecting the spinors thereby we obtain separate equations for eigenvalues $\lambda[\beta,\pm]$ where we suppress

all other quantum numbers previously dealt with,

$$\chi[\lambda[\beta,\pm]]=e^{i(\alpha\pm|\vec{\beta}|/2)}\varphi[\lambda[\beta,\pm]].$$

It is convenient to define two new angles

$$\alpha_\pm=\alpha\pm|\vec{\beta}|/2,$$

and in terms of these angles we can calculate the quark determinant separately for each flavor projection as before. The free energy for each flavor is now a function of four constrained angles

$$F_\pm=F_\pm(\alpha,\beta_+,\beta_0,\beta_-),$$

where we use this suggestive notation instead of β_1,β_2,β_3, and where $\pm$ denotes the isospin projection for the two quark flavors. For a given self-dual domain the total free energy will be a sum

$$F_T(\alpha,\vec{\beta})=F(\alpha_+)+F(\alpha_-),$$

where F is the result from the one-flavor case. Under the assumption that the anomaly provides the entire chiral angular dependence of the determinant, the nonsinglet angles β^a drop out due to the form $2q\arctan[\tan(\alpha)]=2q(\alpha+2n\pi)$. This expresses the known result that the anomaly depends only on the flavor singlet directions or is Abelian. Thus, for an ensemble of domains, the free energy is identical to that for one massless flavor, namely, it depends only on the Abelian angle α. Thus, for $N_f=2$, the $U_A(1)$ direction remains fixed by energy minimization while the $SU(2)_L\times SU(2)_R$ directions represent degeneracies in the space of ground states in the thermodynamic limit.

For $N_f=3$ the boundary condition will now involve the flavor mixing matrix

$$e^{i\beta^a\lambda^a/2}$$

in terms of the Gell-Mann matrices. It is now harder to explicitly diagonalize and project into flavor sectors. Nonetheless the form of the result is clear. The Cartan subalgebra consists of the diagonal generators λ^3 and λ^8. Thus the result of a diagonalization of the argument of the exponential will have the form

$$\beta^a\lambda^a/2\to b^A\lambda^A/2,\ A=3,8,$$

where $b^i=b^i(\beta^a)$, functions of the original nonsinglet angles analogous to $|\vec{\beta}|$ for $N_f=2$. Thus diagonalization will amount to

$$e^{i\beta^a\lambda^a/2}\to\mathrm{diag}(e^{b^3+b^8/\sqrt{3}},e^{-b^3+b^8/\sqrt{3}},e^{-2b^8/\sqrt{3}}).$$

So projection of the combined $U(1)\times SU(3)$ chiral boundary condition will lead to three sets of equations with the eigenvalues depending on the combinations of angles

$$B_1=\alpha+b^3+\frac{1}{\sqrt{3}}b^8,$$

$$B_2=\alpha-b^3+\frac{1}{\sqrt{3}}b^8,$$

$$B_3=\alpha-\frac{2}{\sqrt{3}}b^8,$$

where evidently

$$\sum_i B_i=3\alpha,$$

reflecting ultimately the tracelessness of the generators. The free energy for a given domain will be the sum of three terms

$$F_T=\sum_{i=1}^{3}F(B_i)$$

with F being the same expression evaluated for the one-flavor case. Once again, the assumption of the anomaly means cancellation of the β^a-dependent functions b^A, leaving only the α dependence in the free energy. Once again energy minimization constrains the $U_A(1)$ direction, leaving the $SU(3)_L\times SU(3)_R$ directions unconstrained. Thus for $N_f=3$ one expects eight, not nine, continuous directions in the space of vacua.

The argument for arbitrary N_f is now evident, the key ingredients being the tracelessness of $SU(N_f)$ generators and the specific form of the anomaly for the quark determinant.

VI. ESTIMATION OF MESON MASSES

The consequences of the above realization of chiral symmetries should be seen in the meson spectrum providing the splitting between pseudoscalar and vector mesons and between the pseudoscalar octet and η'.

The source for the difference between the masses of the octet states and η' can be recognized in the drastic difference between correlators of the flavor octet $J^a_{\mathrm{P}}(x)$ and singlet $J_{\mathrm{P}}(x)$ pseudoscalar quark currents as they appear in the domain model,

$$\langle J^a_{\mathrm{P}}(x)J^b_{\mathrm{P}}(y)\rangle=\overline{\langle\langle J^a_{\mathrm{P}}(x)J^b_{\mathrm{P}}(y)\rangle\rangle},$$

$$\langle J_{\mathrm{P}}(x)J_{\mathrm{P}}(y)\rangle=\overline{\langle\langle J_{\mathrm{P}}(x)J_{\mathrm{P}}(y)\rangle\rangle}-\overline{\langle\langle J_{\mathrm{P}}(x)\rangle\rangle\langle\langle J_{\mathrm{P}}(y)\rangle\rangle}. \quad (37)$$

Here double brackets denote integration over quantum fluctuation fields and the overbar means integration over all configurations in the domain ensemble. The second term in the right-hand side (RHS) of the flavor singlet correlator contains two quark loops and is subleading in $1/N_c$ compared with the first one-loop contribution. The second term is entirely determined by the correlation function of the back-

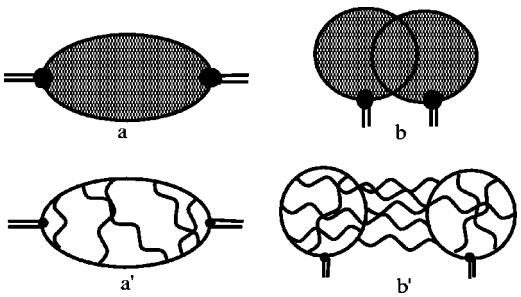

FIG. 2. Diagrammatic representation of two types of contributions to the flavor singlet correlator: (a) and (b) as in the domain model; (a′) and (b′) as in full QCD. The gray background in (a),(b) represents the nonperturbative part of the gluon exchange indicated in diagrams (a′),(b′).

ground gluon field B in the ensemble (8) and is proportional to the quark condensate squared. The analogous two-loop term in the flavor nonsinglet correlator is equal to zero due to the trace over flavor indices. It should be added that the pseudoscalar condensate $\langle\bar{\psi}\gamma_5\psi\rangle$ naturally vanishes since parity is not broken in the ensemble of domains. Thus massless modes can be expected in the nonsinglet channel, but not in the flavor singlet due to the additional term in the correlator. This general structure of correlators is exactly the same as in the instanton liquid model [15] and manifests the mechanism for eta-prime mass generation proposed by Witten in [11] and appreciated in chiral perturbation theory by [16]. The correspondence between domain model correlators to the original QCD diagrams is illustrated in Fig. 2. The gray background denotes averaging over the domain ensemble and is intended to represent the nonperturbative intermediate range part of the gluon exchange in the original QCD diagrams (a′) and (b′). Diagrams (a) and (b) correspond to the first and second terms in the RHS of Eq. (37). The averaging in diagram (b) relates to both quark loops, which is the domain model representation of the exchange between quark loops in (b′) by infinitely many gluons in the original QCD representation. It should be noted that diagrams (a) and (b) in Fig. 2 are the lowest order contributions in the fluctuation gluon fields Q which are treated as perturbations of the background. Higher orders include exchange by gluonic fluctuations in the presence of the domain mean field.

Direct calculation of meson masses within the domain model is not available yet. However, we can estimate the effect of contributions subleading in $1/N_c$ in the flavor singlet pseudoscalar correlator within a calculational scheme that is quite close to the domain model in this respect. This is the main purpose of this section. Simultaneously we will schematically expose the form of the effective action for collective colorless mesonlike modes as are expected to emerge in the domain model and estimate the value of the typical dimensionless parameter BR^2 but now from the meson spectrum. The model that will be used for this purpose is based on the bosonization of a one-gluon exchange interaction between quark currents and in which both quark and gluon propagators are exact solutions in the presence of a background (anti-)self-dual homogeneous gluon field as in [17–19], but here with additional correlations of the type (b) in Fig. 2. In [17–19], as well as the formulation of the model based on a homogeneous gluon field, applications to the calculation of the spectrum of light mesons, their orbital excitations, heavy-light mesons, heavy quarkonia, decay constants, and form factors are given.

In the presence of a homogeneous (anti-)self-dual background field, the quark condensate emerges due to chiral zero modes, but, since there is a continuum of such modes in the homogeneous field, ''an overkill'' occurs [20,21]:

$$m\langle\bar{\psi}\psi\rangle\propto -B^2, \quad m\to 0,$$

and the limit $m\to 0$ cannot be defined properly. However, because of the same zero modes the momentum representation correlators of scalar, pseudoscalar, vector, and axial vector currents have the following limits for $m\to 0$:

$$\tilde{\Pi}_{P/S}\to \mp\frac{B^2}{m^2}F_1(p^2/B),$$

$$\tilde{\Pi}_{V/A}\to \mp BF_2(p^2/B). \tag{38}$$

Such a qualitatively different behavior of correlators becomes manifest already at $m^2/B\sim O(1)$ and leads to a strong splitting of the masses of the corresponding mesons, ensuring light pions and heavy ρ mesons in particular [18] (see also [15]). The fitted values of quark masses in the model correspond to the constituent masses.

The definition of the chiral limit in that model thus cannot be given in terms of quark masses. However, as we discuss below, it is nonetheless possible to define a regime when the calculated pion mass vanishes. The curious side of this approach to the description of chiral properties of the light mesons is that the zero-mode mechanism of condensate formation alone is exploited without any use made of a Nambu-Jona-Lasinio (NJL) or, more generally, Dyson-Schwinger equation (DSE) type mechanism [22]. The inclusion in this model of the additional correlations (b),(b′) of Fig. 2 for the flavor singlet channel enables this approach to also work phenomenologically for $\eta-\eta'$ masses with the chiral limit so defined.

In the domain model studied in the first part of this paper the quark condensate also appears due to specific chiral properties of the (now nonzero) Dirac modes in gluon (domain-like) background fields and not due to a four-fermion interaction. The chiral properties of these low lying modes resemble the properties of zero modes in the homogeneous field model. The condensate diverges as $R\to\infty$ as shown in Fig. 1, much as the condensate in the homogeneous field model diverges as $1/m$. We expect that this dependence on R in the domain model should have a similar effect on meson correlators and masses as does the $1/m$ singularity in the homogeneous field case. The characteristic scale of higher modes is defined by the field strength B rather than the domain radius for $BR^2\gg 1$. Thus one would expect that the heuristic consideration below should be more consistent with the domain model picture if $BR^2\gg 1$.

The difference is that in the domain model flavor chiral symmetry is broken spontaneously, which is not the case in the homogeneous field model. So we should expect a massless pion for massless quarks: the current mass and the chiral limit are well defined, as has been discussed in previous sections. However, a detailed description of the emergence of Goldstone modes is a question of detailed study of correlators and the bound state problem in the domain model, which is still beyond our efforts.

To conclude these preliminary comments, the direct purpose of the following calculations is to demonstrate the (π,K)-η-η' splitting due to the correlations in Fig. 2(b). An auxiliary purpose, justified by the similarity of chiral properties of zero modes in the homogeneous model and nonzero eigenmodes in the domain model, is a demonstration that the pseudoscalar singlet-octet mass splitting occurs simultaneously with a correct description of pseudoscalar-vector meson splitting.

A. Effective action for colorless composite fields

We shall estimate meson masses within the model described by the following partition function:

$$Z=\mathcal{N}\lim_{V\to\infty}\int D\Phi_{\mathcal{Q}} \times\exp\left\{-\frac{B}{2}\frac{h_{\mathcal{Q}}^2}{g^2C_{\mathcal{Q}}}\int dx\Phi_{\mathcal{Q}}^2(x)-\sum_k\frac{1}{k}W_k[\Phi]\right\}, \tag{39}$$

$$1=\frac{g^2C_{\mathcal{Q}}}{B}\tilde{\Gamma}^{(2)}_{\mathcal{Q}Q}(-M_{\mathcal{Q}}^2|B), \tag{40}$$

$$h_{\mathcal{Q}}^{-2}=\frac{d}{dp^2}\tilde{\Gamma}^{(2)}_{\mathcal{Q}Q}(p^2)|_{p^2=-M_{\mathcal{Q}}^2}. \tag{41}$$

The effective action in Eq. (39) is expressed in terms of colorless composite meson fields $\Phi_{\mathcal{Q}}(x)$ with the mass $M_{\mathcal{Q}}$ defined by Eq. (40), where the condensed index $\mathcal{Q}$ denotes isotopic and space-time indices as well as all possible mesonic quantum numbers (isospin, spin parity in the ground state, total momentum, radial quantum number) and k-point nonlocal vertices $\Gamma^{(k)}_{\mathcal{Q}_1\ldots\mathcal{Q}_k}$:

$$W_k[\Phi]=\sum_{\mathcal{Q}_1\cdots\mathcal{Q}_k}h_{\mathcal{Q}_1}\cdots h_{\mathcal{Q}_k}\int dx_1\cdots\int dx_k\Phi_{\mathcal{Q}_1}(x_1)\cdots\Phi_{\mathcal{Q}_k}(x_k)\Gamma^{(k)}_{\mathcal{Q}_1\cdots\mathcal{Q}_k}(x_1,\ldots,x_k|B),$$

$$\Gamma^{(1)}_{\mathcal{Q}_1}=\overline{G^{(1)}_{\mathcal{Q}_1}}, \tag{42}$$

$$\Gamma^{(2)}_{\mathcal{Q}_1\mathcal{Q}_2}=\overline{G^{(2)}_{\mathcal{Q}_1\mathcal{Q}_2}(x_1,x_2)}-\Xi_2(x_1-x_2)\overline{G^{(1)}_{\mathcal{Q}_1}G^{(1)}_{\mathcal{Q}_2}}, \tag{43}$$

$$\Gamma^{(3)}_{\mathcal{Q}_1\mathcal{Q}_2\mathcal{Q}_3}=\overline{G^{(3)}_{\mathcal{Q}_1\mathcal{Q}_2\mathcal{Q}_3}(x_1,x_2,x_3)}-\frac{3}{2}\Xi_2(x_1-x_3)\overline{G^{(2)}_{\mathcal{Q}_1\mathcal{Q}_2}(x_1,x_2)G^{(1)}_{\mathcal{Q}_3}(x_3)} +\frac{1}{2}\Xi_3(x_1,x_2,x_3)\overline{G^{(1)}_{\mathcal{Q}_1}(x_1)G^{(1)}_{\mathcal{Q}_2}(x_2)G^{(1)}_{\mathcal{Q}_3}(x_3)}, \tag{44}$$

$$\Gamma^{(4)}_{\mathcal{Q}_1\mathcal{Q}_2\mathcal{Q}_3\mathcal{Q}_4}=\overline{G^{(4)}_{\mathcal{Q}_1\mathcal{Q}_2\mathcal{Q}_3\mathcal{Q}_4}(x_1,x_2,x_3,x_4)}-\frac{4}{3}\Xi_2(x_1-x_2)\overline{G^{(1)}_{\mathcal{Q}_1}(x_1)G^{(3)}_{\mathcal{Q}_2\mathcal{Q}_3\mathcal{Q}_4}(x_2,x_3,x_4)} -\frac{1}{2}\Xi_2(x_1-x_3)\overline{G^{(2)}_{\mathcal{Q}_1\mathcal{Q}_2}(x_1,x_2)G^{(2)}_{\mathcal{Q}_3\mathcal{Q}_4}(x_3,x_4)}+\Xi_3(x_1,x_2,x_3)\overline{G^{(1)}_{\mathcal{Q}_1}(x_1)G^{(1)}_{\mathcal{Q}_2}(x_2)G^{(2)}_{\mathcal{Q}_3\mathcal{Q}_4}(x_3,x_4)} -\frac{1}{6}\Xi_4(x_1,x_2,x_3,x_4)\overline{G^{(1)}_{\mathcal{Q}_1}(x_1)G^{(1)}_{\mathcal{Q}_2}(x_2)G^{(1)}_{\mathcal{Q}_3}(x_3)G^{(1)}_{\mathcal{Q}_4}(x_4)}, \tag{45}$$

and analogous expressions for the higher vertices. Defining the meson-quark coupling constants $h_{\mathcal{Q}}$ by Eq. (41) provides for the correct residue of the meson propagators at the poles and is known as a compositeness condition [23].

The vertices $\Gamma^{(k)}$ are expressed via quark loops $G^{(n)}_{\mathcal{Q}}$ with n quark-meson vertices,

$$\overline{G^{(k)}_{\mathcal{Q}_1\cdots\mathcal{Q}_k}(x_1,\ldots,x_k)} = \int_\Sigma d\sigma_j \mathrm{Tr}\, V_{\mathcal{Q}_1}(x_1|B^{(j)})S(x_1,x_2|B^{(j)})\cdots V_{\mathcal{Q}_k}(x_k|B^{(j)})S(x_k,x_1|B^{(j)}),$$

$$\overline{G^{(l)}_{\mathcal{Q}_1\cdots\mathcal{Q}_l}(x_1,\ldots,x_l)G^{(k)}_{\mathcal{Q}_{l+1}\cdots\mathcal{Q}_k}(x_{l+1},\ldots,x_k)}$$
$$= \int_\Sigma d\sigma_j \mathrm{Tr}\{V_{\mathcal{Q}_1}(x_1|B^{(j)})S(x_1,x_2|B^{(j)})\cdots V_{\mathcal{Q}_k}(x_l|B^{(j)})S(x_l,x_1|B^{(j)})\}$$
$$\times \mathrm{Tr}\{V_{\mathcal{Q}_{l+1}}(x_{l+1}|B^{(j)})S(x_{l+1},x_{l+2}|B^{(j)})\cdots V_{\mathcal{Q}_k}(x_k|B^{(j)})S(x_k,x_{l+1}|B^{(j)})\}, \quad (46)$$

where the overbar denotes integration over all configurations of the background field with measure $d\sigma_j$. The quark propagator

$$S(x,y) = \exp\left(-\frac{i}{2}x_\mu \hat{B}_{\mu\nu} y_\nu\right) H(x-y),$$

$$\tilde{H}(p) = \frac{1}{2v\Lambda^2}\int_0^1 ds e^{-p^2/2v\Lambda^2}\left(\frac{1-s}{1+s}\right)^{m^2/4v\Lambda^2}$$
$$\times\left[p_\alpha\gamma_\alpha \pm is\gamma_5\gamma_\alpha f_{\alpha\beta}p_\beta + m\left(P_\pm + P_\mp\frac{1+s^2}{1-s^2} - \frac{i}{2}\gamma_\alpha f_{\alpha\beta}\gamma_\beta\frac{s}{1-s^2}\right)\right]$$

is the exact Dirac propagator in the presence of the (anti-) self-dual homogeneous field

$$\hat{B}_\mu(x) = -\frac{1}{2}\hat{n}B_{\mu\nu}x_\nu, \quad \hat{B}_{\mu\nu}\hat{B}_{\mu\rho} = 4v^2\Lambda^4\delta_{\nu\rho},$$

$$f_{\alpha\beta} = \frac{\hat{n}}{v\Lambda^2}B_{\mu\nu}, \quad v = \mathrm{diag}(1/6,1/6,1/3),$$

where we introduced a scale Λ related to the field strength B as

$$\Lambda^2 = \frac{\sqrt{3}}{2}B.$$

For arbitrary orbital momentum l and radial quantum number n the vertex function (more precisely, the vertex differential operator) is factorized into a radial part

$$F_{nl}(s) = \int_0^1 dt t^{l+n}e^{st}, \quad s = \vec{\nabla}^2/\Lambda^2,$$

$$\vec{\nabla}_{ff'} = \xi_f\vec{\nabla} - \xi_{f'}\vec{\nabla}, \quad \xi_f = m_f/(m_f+m_{f'}),$$

$$\vec{\nabla}_\mu = \vec{\partial}_\mu + iB_\mu, \quad \vec{\nabla}_\mu = \vec{\partial}_\mu - iB_\mu \quad (47)$$

and an angular part. In our particular calculation below we will not deal with the excited states. For the explicit form of the angular part of the vertex the reader is referred to [18], where technical details of the derivation of meson-quark vertices $V_{\mathcal{Q}_k}(x_k|B^{(j)})$ and discussion of the approximations and assumptions behind the derivation of the effective action for composite fields can be found. A simplified scalar field model allowing exact implementation of the method has been considered, and a variational procedure for the approximate solution of realistic problems has been formulated in [24]. The relation of this method to the Bethe-Salpeter equation and the nonrelativistic limit are analyzed in [24,25].

Thus the n-point vertex $\Gamma^{(n)}$ includes contributions of two types—the usual one-loop contributions (averaged over the background field) as diagram (a) in Fig. 3 and products of two or more such one-loop terms simultaneously averaged over the background field and multiplied by the corresponding correlators Ξ of the background field, for example as in diagrams (b) and (c) of Fig. 3 for the three-point vertex. In the absence of a background field these additional terms would be just disconnected diagrams and would not appear in the effective action. For the purely constant field B they would correspond to infinite length correlations breaking the cluster decomposition property in the effective action ($\Xi_n \equiv 1$). The idea of domains is implemented in the above expressions by means of finite length correlations of the background field, which ensures cluster decomposition.

The n-point correlation functions Ξ_n of the background field are defined in Eq. (8). In particular, the two-point correlator which will be used below can be written in the explicit form

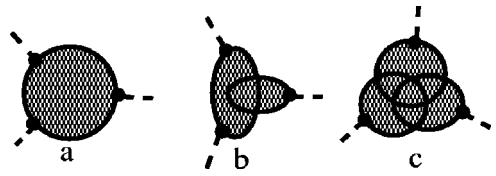

FIG. 3. Diagrammatic representation of the three-point vertex function $\Gamma^{(3)}_{\mathcal{Q}_1\mathcal{Q}_2\mathcal{Q}_3}$. Diagram (a) corresponds to the first term in the RHS of Eq. (44), (b) and (c) to the second and third terms, respectively. Solid lines are quark propagators S in the background field, vertices correspond to nonlocal quark-meson vertices $V_{\mathcal{Q}_i}$, and the dashed lines represent meson fields $\Phi_{\mathcal{Q}_i}$.

$$\Xi_2(x-y)=\frac{N}{V}\int_V dz\,\theta(x-z)\,\theta(y-z)=\frac{2}{3\pi}\phi\left(\frac{(x-y)^2}{4R^2}\right),$$

$$\phi(\rho^2)=\left[\frac{3\pi}{2}-3\arcsin(\rho)-3\rho\sqrt{1-\rho^2}\right.$$
$$\left.-2\rho(1-\rho^2)\sqrt{1-\rho^2}\right]. \quad (48)$$

Geometrically, the correlation function $\Xi_2(x-y)$ is equal to the volume of overlap between spherically symmetric four-dimensional regions determined by the characteristic function θ and central points x, y, normalized to the volume of a single such region.

Now all the elements of the effective action Eq. (39) are fixed: nonlocal meson-quark vertices $V_{\mathcal{Q}_1}(x_1|B^{(j)})$ and quark propagators $S(x_k,x_1|B^{(j)})$ and background field correlators are given in explicit analytical form.

It should be noted here that meson-quark vertices are determined by the gluon propagator in the presence of the background field. In momentum representation the quark propagator, meson-quark vertices, and correlators of the background field are entire functions in the complex momentum plane, which means that quarks and gluons are absent in the model as asymptotic states, which is treated as color confinement. In the momentum representation the vertices $\Gamma^{(n)}$ have no imaginary parts and the probability of a meson to decay into a quark-antiquark pair is zero. As is shown in [17,18], within the model formulated above and clarified in a simplified exactly solvable model in [24], entire propagators and vertices lead to a Regge spectrum of excited bound states represented by composite fields $\Phi_{\mathcal{Q}}$.

The only free parameters of the model are the same as in the domain model discussed in the first part of this paper: the background field strength B, mean domain radius R, strong coupling constant g, and quark masses m_f. The factor $C_{\mathcal{Q}}$ in front of the gauge coupling constant g in Eqs. (39) and (40) is known explicitly:

$$C_{Jnl}=C_J\frac{l+1}{2^l n!(l+n)!},\quad C_{S/P}=\frac{1}{9},\quad C_{S/P}=\frac{1}{18}.$$

The only place where the gauge coupling constant g enters this scheme is the equation for meson masses Eq. (40); the rest of the effective action contains the meson-quark coupling constants calculated by means of Eq. (41).

In the next subsection we present results for the masses of pseudoscalar and vector nonets coming straightforwardly from this formalism with a special emphasis on the η and η'.

B. The masses and decay constants of η and η'

With this representation, the calculation of masses of light mesons and weak decay constants, as performed in [18], is modified only with respect to the η and η' masses. The equations for these masses contain terms with an additional correlation Ξ_2, and this splits them from the remaining light pseudoscalar mesons.

As follows from Eqs. (40) and the second term of Eqs. (42) and (46), the simplest quark loops relevant to the calculation of masses are the constants

$$G^{(1)}_{aP}=-\mathrm{Tr}\,\lambda^a i\gamma_5 F_{00}(x|B^{(j)})S(x,x|B^{(j)}), \quad (49)$$

corresponding to the quark loops in Fig. 2(b). Here a is the flavor index ($a=0,\ldots,8$). In the isosinglet case ($a=0$) this quantity is nonzero. If the s-quark mass is not degenerate with the masses of u and d quarks then $G^{(1)}_{8P}$ is also nonzero. For $a=1,\ldots,7$ the constants are identically equal to zero.

Calculation of $G^{(1)}_{aP}$ is quite simple. The result of the action of the vertex operator $F_{00}(x|B)$ on the quark propagator can be found as follows [in our case $\xi_f=1/2$ in Eq. (47)]:

$$F_{00}(x|B)S(x,x|B)$$
$$=\int_0^1 dt\,\exp\left\{\frac{t}{4\Lambda^2}(\overleftarrow{\nabla}_x-\overrightarrow{\nabla}_y)^2\right\}S(y,x|B)|_{x=y}$$
$$=\int_0^1 dt\int\frac{d^4p}{(2\pi)^4}\tilde{H}(p)e^{-tp^2/\Lambda^2}. \quad (50)$$

Furthermore,

$$\mathrm{Tr}\,i\gamma_5\tilde{H}(p)=\mp\frac{2im}{v\Lambda^2}\int_0^1 ds e^{-sp^2/2v\Lambda^2}\left(\frac{1-s}{1+s}\right)^{m^2/4v\Lambda^2}\frac{s^2}{1-s^2}. \quad (51)$$

Here the sign "$\mp$" relates to self- and anti-self-dual configurations of the vacuum field.

Substitution of Eqs. (51) and (50) in Eq. (49) and integration over the loop momentum p and the parameter t leads to the following integral representation:

$$G^{(1)}_{aP}=\pm i\frac{\Lambda^3}{2\pi^2}\sum_f \lambda^a_{ff}R_f,$$

$$R_f=\sum_v v\frac{m_f}{\Lambda}\int_0^1\frac{dss}{(2v+s)(1-s^2)}\left(\frac{1-s}{1+s}\right)^{m_f^2/4v\Lambda^2}, \quad (52)$$

where the summations over f and v correspond to traces in the flavor and color spaces. As indicated in Eq. (47), v is a diagonal matrix relating to the direction of the vacuum field in color space.

Equation (52) results in the following momentum representation of the two-point correlation function Eq. (42):

$$\Lambda^{-2}\tilde{\Gamma}^{(2)}_{aP,bP}(p^2)=\tilde{\Pi}_{ab}(p^2)=\Pi_{ab}(p^2)-\delta\Pi_{ab}(p^2),$$

where

$$\delta\Pi_{ab}(p^2)=-\frac{8}{3\pi^4}(\Lambda R)^4T^{ab}F(p^2),$$

$$T^{ab}=\sum_{ff'}\lambda^a_{ff}\lambda^b_{f'f'}R_fR_{f'},$$

$$F(p^2)=\int_0^1 dt\sqrt{1-t^2}\int_0^1 ds\,s\cos(\sqrt{4p^2R^2t^2s})\times\left[\frac{3\pi}{2}-3\arcsin\sqrt{s}-(5-2s)\sqrt{s(1-s)}\right],$$

$$T^{00}=\frac{1}{3}(2R_u+R_s)^2,\quad T^{88}=\frac{2}{3}(R_u-R_s)^2,$$

$$T^{08}=\frac{\sqrt{2}}{3}(2R_u+R_s)(R_u-R_s),$$

$$\Pi_{00}=\frac{1}{3}(2\Pi_u+\Pi_s),\quad \tilde{\Pi}_{88}=\frac{1}{3}(\Pi_u+2\Pi_s),$$

$$\Pi_{08}=\frac{\sqrt{2}}{3}(\Pi_u-\Pi_s). \tag{53}$$

The function $\Pi_f(p^2)$ has been calculated in Ref. [18],

$$\Pi_f(p^2)=-\frac{1}{4\pi^2}\mathrm{Tr}_v\int_0^1 dt_1\int_0^1 dt_2\int_0^1 ds_1\int_0^1 ds_2\left(\frac{1-s_1}{1+s_1}\right)^{m_f^2/4v\Lambda^2}\left(\frac{1-s_2}{1+s_2}\right)^{m_f^2/4v\Lambda^2}\times\left[-\frac{p^2}{\Lambda^2}\frac{F_1(t_1,t_2,s_1,s_2)}{\varphi_2^4(t_1,t_2,s_1,s_2)}+\frac{m_f^2}{\Lambda^2}\frac{F_2(s_1,s_2)}{(1-s_1^2)(1-s_2^2)\varphi_2^2(t_1,t_2,s_1,s_2)}+\frac{2v(1-4v^2t_1t_2)F_3(s_1,s_2)}{\varphi_2^3(t_1,t_2,s_1,s_2)}\right]\times\exp\left\{-\frac{p^2}{2v\Lambda^2}\varphi(t_1,t_2,s_1,s_2)\right\},$$

$$\varphi=\frac{\varphi_1(t_1,t_2,s_1,s_2)}{\varphi_2(t_1,t_2,s_1,s_2)},\quad \varphi_1=\frac{1}{2}v(t_1+t_2)[s_1+s_2]+s_1s_2,$$

$$\varphi_2=2v(t_1+t_2)(1+s_1s_2)+(1+4v^2t_1t_2)(s_1+s_2),$$

$$F_1=(1+s_1s_2)\{[s_1+v(t_1+t_2)][s_2+v(t_1+t_2)]+v^2(t_1-t_2)^2s_1s_2\},$$

$$F_2=(1+s_1s_2)^2,\quad F_3=2(1+s_1s_2).$$

The masses of η and η' can be calculated by means of Eqs. (40), which take the forms

$$1+\frac{g^2}{9}\Pi_\eta(-M_\eta^2)=0,\quad 1+\frac{g^2}{9}\Pi_{\eta'}(-M_{\eta'}^2)=0,$$

$$\Pi_\eta=\frac{1}{2}[\tilde{\Pi}_{00}+\tilde{\Pi}_{88}-\sqrt{(\tilde{\Pi}_{00}-\tilde{\Pi}_{88})^2+4\tilde{\Pi}_{08}^2}],$$

$$\tilde{\Pi}_{\eta'}=\frac{1}{2}[\tilde{\Pi}_{00}+\tilde{\Pi}_{88}+\sqrt{(\tilde{\Pi}_{00}-\tilde{\Pi}_{88})^2+4\tilde{\Pi}_{08}^2}],$$

where $\tilde{\Pi}=\Pi-\delta\Pi$ includes both diagrams in Fig. 2. These equations can be written more transparently if we introduce the mixing angle

$$\eta=\eta_8\cos\theta+\eta_0\sin\theta,$$

$$\eta'=\eta_0\cos\theta-\eta_8\sin\theta, \tag{54}$$

where the angle θ is a function of momentum,

$$\tan 2\theta(p^2)=2\tilde{\Pi}_{08}(p^2)/[\tilde{\Pi}_{88}(p^2)-\tilde{\Pi}_{00}(p^2)]. \tag{55}$$

The polarization functions of η and η' and their derivatives with respect to p^2 take the forms

$$\Pi_\eta=\tilde{\Pi}_{88}\cos^2\theta+\tilde{\Pi}_{00}\sin^2\theta+\tilde{\Pi}_{08}\sin 2\theta,$$

$$\Pi_{\eta'}=\tilde{\Pi}_{00}\cos^2\theta+\tilde{\Pi}_{88}\sin^2\theta-\tilde{\Pi}_{08}\sin 2\theta,$$

$$\Pi'_\eta=\tilde{\Pi}'_{88}\cos^2\theta+\tilde{\Pi}'_{00}\sin^2\theta+\tilde{\Pi}'_{08}\sin 2\theta,$$

$$\Pi'_{\eta'}=\tilde{\Pi}'_{00}\cos^2\theta+\tilde{\Pi}'_{88}\sin^2\theta-\tilde{\Pi}'_{08}\sin 2\theta, \tag{56}$$

where for computing derivatives Eq. (55) has been used.

With the values of the parameters

$$m_u=m_d=177.85\ \text{MeV},\quad m_s=400.98\ \text{MeV},$$

$$\sqrt{B}=469.52\ \text{MeV},\quad g=8.94, \tag{57}$$

fitted from the masses of π, ρ, K, and $K^\star$ mesons such that

$$M_\pi=140\ \text{MeV},\quad M_K=496\ \text{MeV},$$

$$f_\pi=129.9\ \text{MeV},\quad f_K=150.8\ \text{MeV},$$

$$M_\rho=M_\omega=770\ \text{MeV},$$

$$M_{K*}=890\ \text{MeV},\quad M_\phi=1035\ \text{MeV}, \tag{58}$$

we find that

$$M_\eta = 640 \text{ MeV}, \quad M_{\eta'} = 950 \text{ MeV},$$

$$h_\eta = 4.72, \quad h_{\eta'} = 2.55$$

for

$$\sqrt{B}R = 1.56. \tag{59}$$

The parameter R was fitted to the η' mass. The domain model value for this dimensionless parameter quoted in the first part of the paper, $\sqrt{B}R = 1.24$, is close to Eq. (59). Thus we see that all features of the spectrum of light vector and pseudoscalar mesons usually associated with chiral symmetries are correctly reproduced by the model quantitatively. The origin of the splitting between the pseudoscalar and vector mesons was discussed in detail in [18]. The new feature is the shift in the masses of η' and η with respect to the other pseudoscalar mesons and their mutual splitting, which occurs here due to the additional contribution of Eq. (53) to their polarization functions. The momentum-dependent mixing angle takes different values at the scale of the η and η' masses:

$$\theta_\eta = \theta(-M_\eta^2) = -19.8°, \quad \theta_{\eta'} = \theta(-M_{\eta'}^2) = 46.1°. \tag{60}$$

It is notable that θ_η coincides with the value of the mixing angle in the naive quark model, while $\theta_{\eta'}$ is completely different from θ_η in both sign and magnitude.

We quote also the result for the weak decay constants of η and η':

$$f_\eta^0 = 4.13 \text{ MeV}, \; f_\eta^8 = 165.7 \text{ MeV}, \; f_\eta^\theta = 154.5 \text{ MeV},$$

$$f_{\eta'}^0 = 288.6 \text{ MeV}, \; f_{\eta'}^8 = 23.67 \text{ MeV},$$

$$f_{\eta'}^\theta = 183.3 \text{ MeV}.$$

These constants are defined by the matrix elements

$$\langle 0 | J_{5\mu}^a(0) | \phi(\mathbf{p}) \rangle = i p_\mu f_\phi^a / \sqrt{2},$$

$$J_{5\mu}^a = \bar{q} \gamma_\mu \gamma_5 t^a q, \quad t^0 = \lambda^0/2, \quad t^8 = \lambda^8/2,$$

and f_ϕ^θ corresponds to the mixings

$$f_\eta^\theta = f_\eta^8 \cos\theta + f_\eta^0 \sin\theta,$$

$$f_{\eta'}^\theta = f_\eta^0 \cos\theta - f_\eta^8 \sin\theta.$$

Here

$$f_\eta^a = h_\eta [f_8^a \cos\theta + f_0^a \sin\theta], \quad f_{\eta'}^a = h_{\eta'} [f_0^a \cos\theta - f_8^a \sin\theta],$$

$$f_0^0 = \frac{1}{3}(2f_u + f_s), \quad f_8^8 = \frac{1}{3}(f_u + 2f_s), \quad f_8^8 = \frac{\sqrt{2}}{3}(f_u - f_s).$$

The function $f_f(-M^2)$ was calculated in [18],

$$f_f = \frac{m_f}{4\pi^2} \sum_v \int_0^1 \int_0^1 \int_0^1 \frac{dt ds_1 ds_2 (1 + s_1 s_2)}{[s_1 + s_2 + 2vt(1 + s_1 s_2)]^3} \times \left[\frac{(1 - s_1)(1 - s_2)}{(1 + s_1)(1 + s_2)} \right]^{m_f^2/4v\lambda^2} \left[2vt + \frac{s_1}{1 - s_1^2} + \frac{s_2}{1 - s_2^2} \right] \times \exp\left(\frac{M^2}{2v\Lambda^2} \Psi(t, s_1, s_2) \right),$$

$$\Psi = \frac{s_1 s_2 + vt(s_1 + s_2)/2}{s_1 + s_2 + 2vt(1 + s_1 s_2)}.$$

As we have already mentioned, the quark masses here should be considered as constituent quark masses. The massless limit is ill defined due to the contribution of zero modes to the quark propagator. However, as is discussed in [18], a peculiar feature is that all the necessary shifts and splittings in the meson spectrum occur explicitly due to the strong (and, for pseudoscalar, scalar, vector, and axial vector states, very different) dependence of the meson masses on the quark masses, which is driven entirely by the zero modes. In order to visualize this picture in a quantitative manner, including now also the η and η', let us consider a regime in the model which can be called ''a chiral limit.''

C. Massless pseudoscalar octet

This limit can be defined in terms of composite meson fields as the condition that the π and K mesons become massless particles. Within the above-formulated meson theory, this requirement is satisfied if the constituent quark masses satisfy the relation

$$m_s = m_d = m_u = m^*$$

and the mass m^* is defined from the equation for the pion mass with $m_\pi = 0$ substituted, that is,

$$1 + \frac{g^2}{9\Lambda^2} \Pi_\pi(0) = 0. \tag{61}$$

Since in this limit the flavor $SU(3)$ becomes an exact symmetry, the kaons are also massless. Furthermore, as follows from Eqs. (53),

$$\Pi_{08} = T^{08} = T^{88} \equiv 0,$$

which means that the η meson is degenerate with the π and K. The mixing angle between η_0 and η_8 is equal to zero and the η' meson corresponds to a pure flavor singlet state. As seen from Eqs. (53),

$$\delta\Pi_{00} \propto T^{00} F(p^2) \neq 0,$$

and the mass of the singlet state is split from the flavor octet states. Vector mesons are massive in this regime. Numerically, one finds

$$m^* = 168.83 \text{ MeV},$$

$$M_\eta = M_\pi = M_K = 0, \; M_{\eta'} = 897 \text{ MeV},$$

$$h_\eta = h_\pi = h_K = 4.28, \; h_{\eta'} = 0.63,$$

$$f_\eta^8 = f_K = f_\pi = 127.76 \text{ MeV}, \; f_{\eta'}^0 = 281.87 \text{ MeV},$$

$$f_\eta^0 = f_{\eta'}^8 = 0,$$

and

$$M_\rho = M_{K^*} = M_\omega = 762 \text{ MeV}, \quad M_\phi = 950 \text{ MeV}.$$

This result displays a typical chiral limit picture with both flavor $SU_R(3) \times SU_L(3)$ and $U_A(1)$ symmetries correctly implemented *de facto*: while the masses of octet states are drastically reduced from their physical values to zero their decay constants are subject to only minor change. Simultaneously we see that the η' does not look like a ''Goldstone'' particle: both its mass and decay constant $f_{\eta'}^0$ are practically unchanged. The vector states are subject to minor change also. For completeness we mention that the scalar and axial vector particles as ground state mesons are absent in the spectrum in this model, but they appear in the hyperfine structure of orbital excitations of vector mesons with quantitatively correct masses [18], which also stays unchanged in the chiral limit described here.

In this picture m^* looks like the condensate part of the constituent quark mass. This impression can be enhanced by estimating the current quark masses and their ratio,

$$\mu_u = m_u - m^* = 9.02 \text{ MeV}, \; \mu_s = m_s - m^* = 232.15 \text{ MeV},$$

$$\mu_s / \mu_u = 25.73.$$

The ratio, which is the only meaningful quantity, almost coincides with the generally accepted value $\mu_s / \mu_u = 25$.

VII. CONCLUSIONS AND DISCUSSION

We have shown that the correlation between the chirality of low lying Dirac modes and the duality of the domainlike background field indeed drives the spontaneous breakdown of flavor chiral symmetry, as was hinted at in [4], and as indicated in lattice calculations [5]. We have also shown that the mechanism generating the η-η' mass splitting is the same as that causing area law confinement in the domain model, namely, the finite range correlations induced by the domain mean field. In more detail, we have extracted the parity odd part of the logarithm of the quark determinant and seen that the axial anomaly is recovered. The chirality properties of the Dirac modes in domains generate the anomaly in this context. We see, however, that in this formulation with domains with baglike boundary conditions, both the symmetric zeta and the asymmetric eta functions are necessary to obtain this result. We then explored the consequences of the anomaly for the realization of chiral symmetry in the domain model. The contribution of the anomaly to the free energy of an ensemble of domains leads to a spontaneous breaking of $Z(2)$ symmetry rather than $U_A(1)$ for one massless fermion flavor. Quark condensation occurs because of the spectral asymmetry coming from the baglike boundary conditions. In the multiflavor case, the Abelian nature of the axial anomaly guarantees that the discrete $Z(2)$ symmetry remains spontaneously broken in addition to the correct continuous nonsinglet $SU(N_f)_L \times SU(N_f)_R$ symmetries. One would thus naively expect only $N_f^2 - 1$ Goldstone bosons based on the number of continuous degenerate directions in the space of ground states of an ensemble of domains.

On this basis we expect massless pions, kaons, and eta mesons in the chiral limit. The domain model manifests correlations Fig. 2(b) in the singlet channel which generates the splitting in η-η' masses via the Witten mechanism. The contribution Fig. 2(b) is entirely driven by the correlators of the background field Eq. (48). Simultaneously, the background field correlators are also entirely responsible for the area law [3]. Thus the origin of both mechanisms is identical. In the $N_c \to \infty$ limit the η' is massless since the contribution of Fig. 2(b) is $1/N_c$ suppressed with respect to Fig. 2(a).

We have seen that the calculational scheme does work well phenomenologically, but the dimensionless parameter turns out to be $BR^2 \approx O(1)$ such that for a self-consistent consideration of meson physics one needs to use the propagators of the domain background field: neglecting boundary conditions inside quark loops is not consistent with $BR^2 \approx O(1)$. There is no clear separation of two scales as has already been observed in the consideration of static parameters of the vacuum—the quark and gluon condensates, the string constant, and the topological susceptibility within the domain model.

Nevertheless, the calculations presented in the final section resemble two features of the domain model we addressed in the first part of the article. The first feature is quite obvious: in both cases the additional contributions to the correlators (polarization functions) for η' and, if $m_u \neq m_s$ also for η, are crucial for their splitting from the other pseudoscalar mesons, thus resolving this aspect of the $U_A(1)$ problem. Certainly, the successful (but not self-consistent) quantitative description provided by the purely homogeneous background field need not *ad hoc* be equally successful in the domain model, and verification of this is one of our first priorities. The second feature is not quite so obvious. The splitting between pseudoscalar and vector meson masses in the case of the purely homogeneous field is determined by the singular behavior of the quark condensate for $m \to 0$ (as mentioned, the condensate diverges in the massless limit due to a continuum of zero modes [20,21]). This singular behavior is not present in the domain model—zero modes do not exist at all and the limit $m \to 0$ is regular. However, a quark condensate is generated in the domain model by the asymmetry in the spectrum of the Dirac operator, and this condensate diverges for $R \to \infty$ as follows from Eqs. (31) and (34) and as shown in Fig. 1, as discussed above. This divergence is expected to play the same role for correlators of the domain model as $m \to 0$ in the homogeneous field, thus generating strong pseudoscalar-vector splitting. The value of the quark condensate given in Eq. (35) corresponds to $R/R_0 = 1$ in Fig. 1. But, unlike the model based on a purely ho-

mogeneous field, the domain model manifests spontaneous breaking of flavor chiral symmetry and hence has the potential to reproduce a genuine picture of the chiral limit. This is only mimicked in the homogeneous field considerations above, although in a surprisingly successful manner.

The zeta function calculation nonetheless remains incomplete, where the contributions that should eliminate the chiral-angle-dependent parity even part of the quark determinant's logarithm need to be calculated. The observation of lack of separation of scales, mentioned above, also means that a more careful study of collective modes within the domain model *per se* is necessary to put the phenomenological results above on a sound footing. In the same context, explicit correlation functions in the domain model would enable a study of the (anomalous) Ward identities and issues [26] related to the realization of Goldstone's theorem (or otherwise) in the $U_A(1)$ sector.

There are two issues naturally related to this work and requiring at least some preliminary comment within the constraints of the calculations realized thus far.

At first superficial glance, the mechanism of quark condensate generation through the asymmetry in the spectrum of the Dirac operator looks to be different from the approach of Banks and Casher [27], where the spectrum is symmetric and the condensate arises due to a finite density of chiral zero modes. However, these seemingly different formulations in fact have more in common. In particular, in the thermodynamic limit the system is characterized by a finite density of low lying (but nonzero) modes which are strongly chiral. Even if for a given fixed domain the spectrum is asymmetric, as indicated by the spectral asymmetry function η, on average all positive and negative nonzero eigenvalues appear in the ensemble in a symmetric way, and neither left nor right chirality modes prevail in the ensemble. This can be seen in the symmetric distribution of the local chirality parameter given in our previous work [4]. The chiral condensate arises due to the existence of a finite density of strongly chiral eigenmodes both in the Banks-Casher formulation and in the model under consideration. The difference is that, in the domain model the corresponding eigenvalues are nonzero in the thermodynamic limit and none of the fermionic modes are purely chiral; rather, they can be characterized by their average chirality with a definite sign correlated with the duality of the mean gluonic field in the domain: the lower the Dirac operator eigenmode the closer this average chirality to ± 1. Thus, we would take the liberty of saying that the domain model gives a ''smeared'' realization of the Banks-Casher scenario.

Another interesting question inspired by the chiral boundary condition used in the model is the manifestation or otherwise of features seen in chiral bag models of the nucleon. How much is in common here beyond the similar boundary condition? There is no simple answer to this question yet. We recall that the domain model is formulated in Euclidean four-dimensional space, colorless hadrons (if any) are not associated with domains themselves but are anticipated to arise as collective excitations of quantum fluctuations of quark (and possibly gluon) fields in the domain ensemble. The description of colorless hadrons requires analytical continuation to physical Minkowski space. Quark and gluon fluctuations in this approach are localized in both space and time: no asymptotic particlelike states can be associated with them. The model requires substantial use of methods of nonlocal quantum field theory. Various issues related to quantization, unitarity, causality, Froissart-type bounds at high energies, and interpetation of nonlocal fields as fluctuations localized in space and time can be found in [23,24,28–30]. The nonlocality appears here primarily due to the presence of strong background gluon fields, which eliminate the pole in the momentum space quark propagator [17,18,31], rendering it an entire analytical function. The nature of colored fluctuations as localized in space and time prohibits a straightforward resolution in the domain model of the manifestation of such interesting features as baryon number fractionalization in chiral bags [32]. This phenomenon appears due to asymmetry (and a corresponding η invariant) in the spectrum of the Dirac Hamiltonian, rather than the Euclidean Dirac operator, after a rearrangement of energy levels in the solitonic background chiral bag. There is no automatic one-to-one correspondence between phenomena in the domain model and those of the chiral bag model for the nucleon. In particular, the answer to the question of baryon number is intimately connected to the analytical properties of the propagators (for example, see [33]) and thus to the mode of dynamical confinement and the realization of hadrons as propagating excitations in the domain ensemble, the subject of further work.

ACKNOWLEDGMENTS

S.N.N. was supported by the DFG under contract SM70/1-1 and, partially, by RFBR grant 01-02-1720. A.C.K. is supported by a grant of the Australian Research Council. We acknowledge the hospitality of the Institute for Theoretical Physics III, University of Erlangen-Nuremberg, where substantial parts of this work were done. In particular, we acknowledge fruitful discussions with Frieder Lenz, Michael Thies, Lorenz von Smekal, Jan Pawlowski, and Andreas Schreiber. We also thank G. V. Efimov for numerous discussions and explanations, K. Kirsten, G. Dunne, and S. Bilson-Thompson.

APPENDIX: EXPANSION OF KUMMER FUNCTIONS

1. Asymptotic form of Kummer function $M(k^2x^2/(4z),k+1,z)$ for $k \gg 1$, z,x fixed

We use the representation [34]

$$M(a/4z,k+1,z)=\frac{k!}{\Gamma(a/4z)}\int_0^\infty dt t^{a/4z-1}(zt)^{-k/2}e^{-t}I_k(2\sqrt{zt})$$

and change the integration variable $2\sqrt{zt}=s$, giving

$$M(a/4z,k+1,z)=\frac{k!z^{-a/4z}2^{k+1-a/2z}}{\Gamma(a/4z)} \times \int_0^\infty ds s^{a/2z-k-1}e^{-s^2/4z}I_k(s).$$

The asymptotic behavior of

$$\mathcal{M}_k = \int_0^\infty ds s^{a/2z-k-1} e^{-s^2/4z} I_k(s)$$

at $a \propto k^2$, $k \gg 1$ can be found by the saddle point method. Denoting $\alpha = a/2z$, $\zeta = 2z$, and $f(s) = [1-(k+1)/\alpha]\ln(s) - s^2/2\alpha\zeta$, we arrive at

$$\mathcal{M}_k = \int_0^\infty ds e^{\alpha f(s)} I_k(s)$$

with $f(s)$ having a maximum at

$$s_0 = \sqrt{\zeta(\alpha-k-1)}.$$

Expanding the exponent about the saddle point and using the addition theorem

$$\left(\frac{z_1 - z_2 e^{-i\phi}}{z_1 - z_2 e^{i\phi}}\right)^\nu I_\nu(\omega) = \sum_{n=-\infty}^{\infty} (-1)^n I_n(z_2) I_{\nu+n}(z_1) e^{in\phi},$$

$$\omega = \sqrt{z_1^2 + z_2^2 - 2z_1 z_2 \cos(\phi)}$$

with $\phi = 0$ and π, one obtains the following representation:

$$\begin{aligned} M(a/4z, k+1, z) &= \sqrt{2\pi z}\, \frac{k! z^{-a/4z} 2^{k+1-a/2z}}{\Gamma(a/4z)} \\ &\times [a - 2z(k+1)]^{a/4z-(k+1)/2} e^{-a/4z+(k+1)/2} e^{z/4} \\ &\times \sum_{n=-\infty}^{\infty} I_{2n+k}(s_0) I_n(z/4) \\ &\times [1 + W_1(x,z,n)/k + W_2(x,z,n)/k^2] \\ &+ \sum_{n=-\infty}^{\infty} I_{2n+k+1}(s_0) I_n(z/4) \frac{W_3(x,z)}{k}, \end{aligned} \tag{A1}$$

$$W_1 = \frac{z(z-2n+3)}{6x^2},$$

$$\begin{aligned} W_2 = \frac{z}{72x^4}[&(27z - 8zn + z^3 + 15z^2 + 4zn^2)\sqrt{1+x^2} + 8zn^2x^2 \\ &- 12x^2 + 15z^2 - 9zx^2 + 2z^2nx^2 + 8n^3x^2 + z^3x^2 + 4z^2x^2 \\ &- 56zn + 27z - 48n^2x^2 + 46nx^2 + 26znx^2 + 4zn^2 + z^3], \end{aligned}$$

$$W_3 = \frac{z(z+3)}{6x},$$

$$s_0 = \sqrt{a - 2z(k+1)}, \quad a = k^2x^2, \quad x = t\rho,$$

and calculation of the asymptotic form of M is reduced to the asymptotic decomposition of $I_{2n+k}(s_0)$ and $I_{2n+k+1}(s_0)$ for $k \gg n$.

Decomposition of the factors in front of the sum in Eq. (A1) at $k \gg 1$ gives

$$\begin{aligned} &\frac{k! z^{-a/4z} 2^{k+1-a/2z}}{\Gamma(a/4z)} [a - 2z(k+1)]^{a/4z-(k+1)/2} \\ &\quad \times e^{-a/4z+(k+1)/2} e^{z/4} \sqrt{2\pi z} \\ &= \frac{k! 2^k}{(kx)^k} e^{z/4 + z/2x^2} \left[1 + \frac{z(3x^2+z)}{3x^4 k} \right. \\ &\quad \left. + \frac{z(3x^6 + 27x^4 z + 12x^2 z^2 + z^3)}{18x^8 k^2} + O(1/k^3)\right]. \end{aligned}$$

The representation

$$I_\nu(s_0) = \frac{1}{\sqrt{\pi}} \frac{s_0^\nu}{2^\nu \Gamma(\nu + 1/2)} \int_{-1}^{1} dt e^{-s_0 t} (1-t^2)^{\nu-1/2}$$

is now suitable for determining an asymptotic decomposition of the $I_{2n+k}(s_0)$, again by means of the saddle point approximation. With

$$g_1(x,n,z) = -\frac{8z^2 + 4x^2 z(2+4n+z) + x^4(-1+16n^2+8z)}{8x^4\sqrt{1+x^2}},$$

$$\begin{aligned} g_2(x,n,z) &= \frac{[8z^2 + 4x^2 z(2+4n+z) + x^4(-1+16n^2+8z)]^2}{128x^8(1+x^2)} \\ &- \frac{1}{24(1+x^2)^{3/2}x^6}\{32z^3 + 48x^2z^2(1+n+z) \\ &+ x^6[-1+6n-32n^3-3z+48n(1+n)z+24z^2] \\ &+ 12x^4 z[z(6+z) + n(4+6z)]\}, \end{aligned}$$

and

$$h_1(x,n,z) = \frac{2(x^2-2)\sqrt{1+x^2} - 5}{24(1+x^2)^{3/2}},$$

$$\begin{aligned} h_2(x,n,z) = \frac{1}{1152(1+x^2)^3}[&-8 - 68x^2 - 720z + 480n \\ &- 960x^2 n)\sqrt{1+x^2} + 17 - 144x^2 + 276x^4 \\ &+ 52x^6 + 384n - 576x^2 n - 1152x^4 n - 192x^6 n \\ &- 576zx^2 - 576z], \end{aligned}$$

we obtain the following full expression for the asymptotics of the Kummer function up to $O(1/k^2)$:

$$
\begin{aligned}
M(a/4z,k+1,z) = {} & \frac{k!2^k}{(kx)^k}\frac{1}{\sqrt{2\pi k}}\frac{1}{(1+x^2)^{1/4}}\exp\left\{k\sqrt{x^2+1}+k\ln\left(\frac{x}{1+\sqrt{x^2+1}}\right)\right\}\exp\left\{z/4+z/2x^2-z\frac{\sqrt{x^2+1}}{x^2}\right\} \\
& \times\left[1+\frac{z(3x^2+z)}{3x^4k}+\frac{z(3x^6+27x^4z+12x^2z^2+z^3)}{18x^8k^2}+O(1/k^3)\right]\sum_{n=-\infty}^{\infty} I_n(z/4)\left(\frac{x}{1+\sqrt{x^2+1}}\right)^{2n} \\
& \times\left\{\left[1+\frac{2z+1-4n}{4(1+x^2)k}+\frac{16n^2(3-2x^2)+8n(2x^2-3-10z)+16zx^2+36z-2x^2+20z^2+3}{32(1+x^2)^2k^2}\right]\right. \\
& \times\left[1+\left(\frac{1}{24}-2n^2\right)\frac{1}{k}+\left(\frac{1}{1152}-\frac{n}{12}-\frac{n^2}{12}+\frac{4n^3}{3}+2n^4\right)\frac{1}{k^2}\right] \\
& \times\left[1+\frac{16n^2-1}{8k}+\frac{768n^4-512n^3-96n^2+96n-13}{384k^2}\right]\left[1+\frac{g_1(x,n,z)}{k}+\frac{g_2(x,n,z)}{k^2}\right] \\
& \times\left[1+\frac{h_1(x,n,z)}{k}+\frac{h_2(x,n,z)}{k^2}\right]\left[1+\frac{W_1(x,n,z)}{k}+\frac{W_2(x,n,z)}{k^2}\right] \\
& +\frac{z(z+3)}{6k(1+\sqrt{1+x^2})}\left[1+\frac{2z-1-4n}{4(1+x^2)k}\right]\left[1+\left(\frac{1}{24}-2(n+1/2)^2\right)\frac{1}{k}\right]\left[1+\frac{16(n+1/2)^2-1}{8k}\right] \\
& \left.\times\left[1+\frac{g_1(x,n+1/2,z)}{k}\right]\left[1+\frac{h_1(x,n+1/2,z)}{k}\right]+O(1/k^3)\right\}.
\end{aligned}
$$

The series over n can now be resummed in terms of the generating function of Bessel functions and its derivatives,

$$
\sum_{n=-\infty}^{\infty} v^n I_n(u) = \exp\left\{\frac{u}{2}\left(v+\frac{1}{v}\right)\right\},
$$

$$
\sum_{n=-\infty}^{\infty} n^l v^n I_n(u) = \left[v\frac{d}{dv}\right]^l \exp\left\{\frac{u}{2}\left(v+\frac{1}{v}\right)\right\},
$$

where

$$
u = z/4, \quad v = \left(\frac{x}{1+\sqrt{x^2+1}}\right)^2, \quad l = 0,1,2,3,4.
$$

Moreover, the presence of the factor

$$
\exp\left\{z/4+z/2x^2-z\frac{\sqrt{x^2+1}}{x^2}\right\}
$$

allows further simplification,

$$
\exp\left\{z/4+z/2x^2-z\frac{\sqrt{x^2+1}}{x^2}\right\}\sum_{n=-\infty}^{\infty}\left(\frac{x}{1+\sqrt{x^2+1}}\right)^{2n} I_n(z/4) = \exp\left\{\frac{z}{2}\frac{\sqrt{x^2+1}-1}{\sqrt{x^2+1}+1}\right\}.
$$

The remaining formulas required can be obtained by differentiation. The final result is then

$$M(a/4z,k+1,z)=\frac{k!2^k}{(kx)^k}\frac{1}{\sqrt{2\pi k}}\frac{1}{(1+x^2)^{1/4}}\exp\left\{k\sqrt{x^2+1}+k\ln\left(\frac{x}{1+\sqrt{x^2+1}}\right)\right\}$$
$$\times\exp\left\{\frac{z}{2}\frac{\sqrt{x^2+1}-1}{\sqrt{x^2+1}+1}\right\}\left[1+\frac{M_1(x,z)}{k}+\frac{M_2(x,z)}{k^2}+O(1/k^3)\right],$$

where

$$M_1(x,z)=-\frac{y(5y^4+(-12z+10)y^3+(12z^2+2-24z)y^2+(-8z^2+12z-6)y+24z-4z^2-3)}{24(y+1)^2}$$

and

$$M_2(x,z)=\frac{y^2}{1152(y+1)^4}[385y^8+(-840z+1540)y^7+(1848+840z^2-3360z)y^6+(-308+3040z^2-4584z-480z^3)y^5$$
$$+(144z^4-2306-1152z^3+3304z^2-1200z)y^4+(-1408z^2-192z^4+3336z-1524+768z^3)y^3+(24-32z^4$$
$$+1344z^3+4128z-4456z^2)y^2+(-1632z^2+324+2088z+64z^4-288z^3)y+16z^4+432z-192z^3+312z^2+81]$$

with

$$y=\frac{1}{\sqrt{x^2+1}}.$$

For the particular case $z=0$ we get

$$M_1(x,0)=-\frac{y(5y^2-3)}{24}$$

and

$$M_2(x,0)=\frac{y^2}{1152}[385y^4-462y^2+81],$$

which reproduce the known asymptotic formulas [35]. This, as well as cancellation of powers of y in the denominators of M_i, gives a quite reliable criterion for correctness of the expression obtained.

2. Asymptotic form of the Kummer function $M(k^2x^2/4z+1,k+2,z)$ for $k\gg1$, z,x fixed

Computations analogous to those of the previous section lead to the result

$$M(k+1+a/4z,k+2,z)=\frac{k!2^k}{(kx)^k}\frac{1}{\sqrt{2\pi k}}\frac{1}{(1+x^2)^{1/4}}\exp\left\{k\sqrt{x^2+1}+k\ln\left(\frac{x}{1+\sqrt{x^2+1}}\right)\right\}$$
$$\times\exp\left\{\frac{z}{2}\frac{\sqrt{x^2+1}-1}{\sqrt{x^2+1}+1}\right\}\left[M_0(x)+\frac{M_1(x,z)}{k}+\frac{M_2(x,z)}{k^2}+O(1/k^3)\right],$$

where

$$M_0(x)=\frac{2y}{1+y},$$

$$M_1(x,z)=-\frac{y[5y^5+(-12z+22)y^4+(-48z+38+12z^2)y^3+(-36z+6-8z^2)y^2+(-39-4z^2)y-24]}{12(y+1)^3}$$

and

$$M_2(x,z)=\frac{y^2}{576(y+1)^5}[385y^9+(-840z+2380)y^8+(-5040z+6048+840z^2)y^7+(-12744z+7636-480z^3+4480z^2)y^6$$
$$+(9160z^2+144z^4-16896z-1728z^3+3478)y^5+(-3660-192z^4+6272z^2-10296z)y^4+(-7440-32z^4$$
$$-1192z^2+1728z^3+1008z)y^3+(-1728z^2-5892+64z^4+480z^3+4680z)y^2+(1728z+16z^4-2439+408z^2)y$$
$$-432+192z^2]$$

with $y=1/\sqrt{x^2+1}$.

3. Asymptotic form of Kummer function $M(-k^2x^2/4z,k+1,-z)$ for $k\gg 1$, z,x fixed

Use of previous calculations can be maximized by writing the function to be decomposed as

$$M(-a/4z,k+1,-z)=e^{-z}M(a/4z+k+1,k+1,z)$$
$$=\frac{k!z^{-a/4z}2^{k+1-a/2z}}{\Gamma(a/4z)}\frac{(4z)^{-k-1}\Gamma(a/4z)}{\Gamma(a/4z+k+1)}$$
$$\times e^{-z}\int_0^\infty ds s^{a/2z+k+1}e^{-s^2/4z}I_k(s).$$

The final result is

$$M(-a/4z,k+1,-z)=e^{-z}M(a/4z+k+1,k+1,z)$$
$$=\frac{k!2^k}{(kx)^k}\frac{1}{\sqrt{2\pi k}}\frac{1}{(1+x^2)^{1/4}}\exp\left\{k\sqrt{x^2+1}+k\ln\left(\frac{x}{1+\sqrt{x^2+1}}\right)\right\}\exp\left\{-\frac{z}{2}\frac{\sqrt{x^2+1}-1}{\sqrt{x^2+1}+1}\right\}$$
$$\times\left[1+\frac{M_1(x,z)}{k}+\frac{M_2(x,z)}{k^2}+O(1/k^3)\right]$$

where

$$M_1(x,z)=-\frac{y[5y^4+(12z+10)y^3+(12z^2+2+24z)y^2+(-8z^2-12z-6)y-24z-4z^2-3]}{24(y+1)^2}$$

and

$$M_2(x,z)=\frac{y^2}{1152(y+1)^4}[385y^8+(840z+1540)y^7+(840z^2+1848+3360z)y^6+(-308+3040z^2+480z^3+4584z)y^5$$
$$+(1152z^3-2306+1200z+144z^4+3304z^2)y^4+(-1408z^2-192z^4-3336z-1524-768z^3)y^3+(24-4456z^2$$
$$-1344z^3-32z^4-4128z)y^2+(-2088z+324+288z^3+64z^4-1632z^2)y+16z^4+192z^3+81+312z^2-432z]$$

with $y=1/\sqrt{x^2+1}$.

4. Asymptotic form of Kummer function $M(-k^2x^2/(4z),k+2,-z)$ for $k\gg 1$, z fixed

The relation of $M(-k^2x^2/(4z),k+2,-z)$ to $M(-k^2x^2/(4z),k+1,-z)$ is analogous to that of $M(k^2x^2/(4z)+1,k+2,z)$ to $M(k^2x^2/(4z),k+1,z)$; thus the calculation is similar to that in Sec. A 3. The result is

$$M(-a/4z,k+2,-z)=e^{-z}M(k+2+a/4z,k+2,z)$$
$$=\frac{k!2^k}{(kx)^k}\frac{1}{\sqrt{2\pi k}}\frac{1}{(1+x^2)^{1/4}}\exp\left\{k\sqrt{x^2+1}+k\ln\left(\frac{x}{1+\sqrt{x^2+1}}\right)\right\}$$
$$\times\exp\left\{-\frac{z}{2}\frac{\sqrt{x^2+1}-1}{\sqrt{x^2+1}+1}\right\}\left[M_0(x)+\frac{M_1(x,z)}{k}+\frac{M_2(x,z)}{k^2}+O(1/k^3)\right]$$

where

$$M_0(x)=\frac{2y}{1+y},$$

$$M_1(x,z)=-\frac{y[5y^5+(12z+22)y^4+(48z+12z^2+38)y^3+(6-8z^2-12z)y^2+(-4z^2-48z-39)y-24]}{12(y+1)^3},$$

and

$$M_2(x,z)=\frac{y^2}{576(y+1)^5}[385y^9+(2380+840z)y^8+(5040z+6048+840z^2)y^7+(4480z^2+7636+12264z+480z^3)y^6$$
$$+(3478+1728z^3+8008z^2+144z^4+13152z)y^5+(-2376z-1792z^2-1152z^3-192z^4-3660)y^4$$
$$+(-19056z-32z^4-11560z^2-2112z^3-7440)y^3+(-2880z^2+672z^3-13032z-5892+64z^4)y^2$$
$$+(384z^3-2439+864z+2712z^2+16z^4)y-432+192z^2+2304z]$$

with

$$y=\frac{1}{\sqrt{x^2+1}}.$$

[1] For example, vortices. Some references are P. de Forcrand and M. D'Elia, Phys. Rev. Lett. **82**, 4582 (1999); J. Greensite and S. Olejnik, Phys. Rev. D **67**, 094503 (2003); H. Reinhardt, Nucl. Phys. **B628**, 133 (2002); M. Engelhardt, *ibid.* **B638**, 81 (2002); P. de Forcrand and L.v. Smekal, Phys. Rev. D **66**, 011504(R) (2002).

[2] P. van Baal, in *At the Frontier of Particle Physics*, edited by M. Shifman (World Scientific, Singapore, 2001), Vol. 2, pp. 760–821.

[3] A.C. Kalloniatis and S.N. Nedelko, Phys. Rev. D **64**, 114025 (2001).

[4] A.C. Kalloniatis and S.N. Nedelko, Phys. Rev. D **66**, 074020 (2002).

[5] R.G. Edwards and U.M. Heller, Phys. Rev. D **65**, 014505 (2002); T. De Grand and A. Hasenfratz, *ibid.* **65**, 014503 (2002); I. Hip *et al.*, *ibid.* **65**, 014506 (2002); T. Blum *et al.*, *ibid.* **65**, 014504 (2002); C. Gattringer *et al.*, Nucl. Phys. **B618**, 205 (2001); **B617**, 101 (2001).

[6] S. Deser, L. Griguolo, and D. Seminara, Phys. Rev. Lett. **79**, 1976 (1997).

[7] A. Wipf and S. Duerr, Nucl. Phys. **B443**, 201 (1995).

[8] L. Bergamin and P. Minkowski, hep-th/0003097; M. Leibundgut and P. Minkowski, Nucl. Phys. **B531**, 95 (1998).

[9] N.K. Nielsen, Nucl. Phys. **B120**, 212 (1977).

[10] P. Minkowski, Nucl. Phys. **B177**, 203 (1981).

[11] E. Witten, Nucl. Phys. **B156**, 269 (1979); G. Veneziano, *ibid.* **B159**, 213 (1979).

[12] M. Bordag, E. Elizalde, and K. Kirsten, J. Math. Phys. **37**, 895 (1996); K. Kirsten, *Spectral Functions in Mathematics and Physics* (Chapman & Hall/CRC Press, Boca Raton, FL, 2001); for a recent application, see C.G. Beneventano, E.M. Santangelo, and A. Wipf, J. Phys. A **35**, 9343 (2004).

[13] E. Elizalde, *Ten Physical Applications of Spectral Zeta Functions*, Vol. M35 of Lecture Notes in Physics (Springer-Verlag, Berlin, 1995).

[14] K. Fujikawa, Phys. Rev. D **21**, 2848 (1980); **22**, 1499(E) (1980).

[15] Th. Schafer and E. Shuryak, Rev. Mod. Phys. **70**, 323 (1998).

[16] See, for example, S.R. Sharpe, Phys. Rev. D **41**, 3233 (1990); C.W. Bernard and M.F. Golterman, *ibid.* **46**, 853 (1992). Some more recent applications of this include R.D. Young *et al.*, *ibid.* **66**, 094507 (2002); S.J. Dong *et al.*, hep-lat/0304005.

[17] G.V. Efimov and S.N. Nedelko, Phys. Rev. D **51**, 176 (1995).

[18] Ja.V. Burdanov, G.V. Efimov, S.N. Nedelko, and S.A. Solunin, Phys. Rev. D **54**, 4483 (1996).

[19] Ja.V. Burdanov, G.V. Efimov, S.N. Nedelko, and S.A. Solunin, hep-ph/9806478.
[20] M.S. Dubovikov and A.V. Smilga, Nucl. Phys. **B185**, 109 (1981).
[21] G.V. Efimov and S.N. Nedelko, Eur. Phys. J. C **1**, 343 (1998).
[22] The difference between the NJL or DSE and instantonlike (zero mode) mechanisms has been discussed in recent work by P. Faccoli and T.A. De Grand, Phys. Rev. Lett. **91**, 182001 (2003), where a specific combination of scalar and pseudoscalar correlators has been used to test the character of chiral symmetry realization in lattice QCD.
[23] G.V. Efimov and M.A. Ivanov, *The Quark Confinement of Hadrons* (IOP, Bristol, 1993); A. Salam, Nuovo Cimento **25**, 224 (1965); S. Weinberg, Phys. Rev. **130**, 776 (1963); K. Hayashi *et al.*, Fortschr. Phys. **15**, 625 (1967).
[24] G.V. Efimov and G. Ganbold, Phys. Rev. D **65**, 054012 (2002).
[25] G.V. Efimov, hep-ph/0304194.
[26] See both R.J. Crewther, in *Field Theoretical Methods in Particle Physics*, edited by W. Rühl, NATO Advanced Study Institute Series Vol. 55B (Plenum, New York, 1980), p. 529, and G. 't Hooft, Phys. Rep. **142**, 357 (1986), for a thorough list of references on this issue.
[27] T. Banks and A. Casher, Nucl. Phys. **B169**, 103 (1980).
[28] G.V. Efimov, Theor. Math. Phys. **128**, 1169 (2001); V.A. Alebastrov and G.V. Efimov, Commun. Math. Phys. **31**, 1 (1973); **38**, 11 (1974); G.V. Efimov and O.A. Mogilevsky, Nucl. Phys. **B44**, 541 (1972); G.V. Efimov, *Nonlocal Interactions of Quantized Fields* (Nauka, Moscow, 1977) (in Russian).
[29] V.Ya. Fainberg and M.A. Soloviev, Teor. Mat. Fiz. **93**, 514 (1992) [Theor. Math. Phys. **93**, 1438 (1992)]; Ann. Phys. (N.Y.) **113**, 421 (1978); Commun. Math. Phys. **57**, 149 (1977).
[30] R. Alkofer and L. von Smekal, Phys. Rep. **353**, 281 (2001).
[31] H. Leutwyler, Phys. Lett. **96B**, 154 (1980).
[32] A.J. Niemi and G.W. Semenoff, Phys. Rep. **135**, 99 (1986).
[33] K.W. Mak, Phys. Rev. D **49**, 6939 (1994); A.N. Sisakian, O.Yu. Shevchenko, and S.B. Solganik, Nucl. Phys. **B518**, 455 (1998).
[34] W. Magnus *et al.*, *Formulas and Theorems for the Special Functions of Mathematical Physics* (Springer-Verlag, Berlin, 1966).
[35] For expansion of Bessel functions see *Handbook of Mathematical Functions*, edited by M. Abramowitz and I. Stegun (Dover Publications, New York, 1968), Eq. (9.7.7).